SCIENCE OF TSUNAMI HAZARDS

The International Journal of The Tsunami Society

OBJECTIVE: **The Tsunami Society** publishes this journal to increase and disseminate knowledge about tsunamis and their hazards.

DISCLAIMER: Although these articles have been technically reviewed by peers, **The Tsunami Society** is not responsible for the veracity of any statement, opinion or consequences.

Submit manuscripts of articles, notes or letters to the Editor. If an article is accepted for publication the author(s) must submit a camera ready manuscript in the journal format. A voluntary $30.00 page charge for Tsunami Society members, $50.00 for non-members will include 50 reprints.

SUBSCRIPTION INFORMATION: Price per copy $20.00 USA

Permission to use figures, tables and brief excerpts from this journal in scientific and educational works is hereby granted provided that the source is acknowledged.

TSUNAMI FROM ASTEROID AND COMET IMPACTS: THE VULNERABILITY OF EUROPE

Jack G. Hills, M. Patrick Goda,
Mail Stop B288
Theoretical Division
Los Alamos National Laboratory
Los Alamos, N.M. 87545, U.S.A.

ABSTRACT

Tsunami is probably the most serious form of damage caused by stony asteroids with diameters between about 200 meters and 2 km. Smaller ones dissipate most of their energy in the atmosphere while larger ones eject enough dust above the atmosphere to produce darkness that lasts for months, which may cause more deaths than a tsunami. Asteroids larger than 200 meters in diameter hit Earth about every 3000 to 5000 years, so the probability of one impacting in a given human lifetime is about 2-3%. In the absence of wave dispersion, even an asteroid 200 meters in diameter impacting in mid Atlantic would produce tsunami several meters high on either side of the ocean. Using a tsunami propagation and runup code, we find that an asteroid 5 kilometers in diameter falling in the mid Atlantic produces tsunami that inundate the upper two-thirds of the Eastern United States to the foothills of the Appalachians. In Europe, the damage is less dramatic: The most vulnerable area is the Spain-Portugal peninsula. It is being thrust into the Atlantic by plate tectonics, so it has little continental shelf, which is ideal for producing large tsunami runups. The same impactor that causes runups in the Eastern United States to the Appalachians causes runups to the mountains of this peninsula. The situation in Northern Europe is more favorable. The extensive, shallow continental shelf around the British Isles reflects much of the tsunami energy back into the Atlantic. The UK and the continent facing it are relatively protected from tsunami.

I. INTRODUCTION

Asteroid and comet impacts cause a variety of damage: blastwaves, fires, craters and earthquakes on land and tsunami at sea (Hills and Goda 1993, hereafter referred to as HG, and Hills and Goda 1998). If the impactor is more than 1 km in diameter, it ejects enough dust above the atmosphere to produce global darkening. Global darkening over a period of months could cause mass starvation in developing countries. The work of HG showed that tsunami is the most significant form of damage for objects smaller than this threshold for global darkening.

Fig. 1 (from HG) shows the full height of tsunami in deepwater (before they hit land) at 1000 miles from the impact point as a function of asteroid radius and impact velocity. (Heights above sea level are half these values.) These calculations were based on the kinetic energy at which the asteroid impacts the ocean and the relationship between energy released and tsunami height found from nuclear explosive tests in the Pacific (Glasstone and Dolan 1977). When tsunami run onto land, their heights at some locales can be up to an order of magnitude higher than they were in deep water. The average runup along an entire coast is perhaps three fold, but it depends greatly on local conditions.

We see from Fig. 1 that significant tsunami are only produced if the asteroid radius exceeds 100 meters. Objects this size impact the ocean every 3000 to 5000 years. The tsunami height rises rapidly with asteroid radius above this threshold. The impact of an asteroid just over 100 meters in radius hitting the atmosphere at the typical impact velocity of 20 km/s produces tsunami about 5 meters above sea level at 1000 km from the impact point while one 1 km in diameter produces tsunami about 35 meters above sea level. If the impact occurs in mid Atlantic, it would (in the absence of wave dispersion) produce tsunami about a third this height just before the wave comes ashore. However, the average runup as it comes ashore is about three fold, so, e.g., an asteroid 1 km in diameter falling in the MidAlantic might be expected to produce tsunami with average runup heights of about 35 meters on either side of the ocean.

The smaller the asteroid, the smaller the crater it produces, and the shorter the wavelength of the tsunami. At short enough wavelengths wave dispersion may be important in reducing the tsunami height at large distance (many wavelengths) from the impact point. To calculate the effect of wave dispersion on tsunami height will require solution of the Navier Stokes

Soft Stone
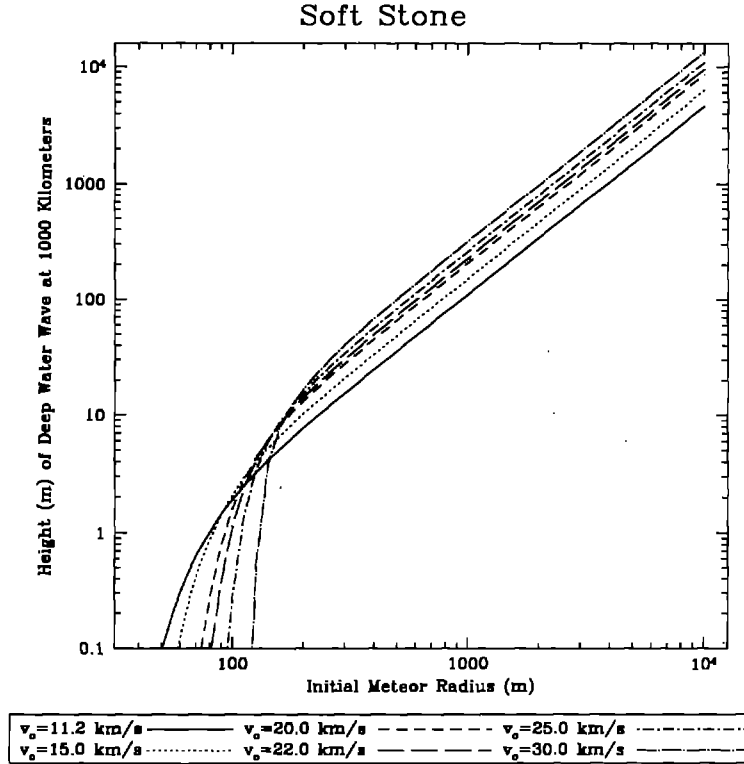
Figure 1: Full height of tsunami in deep water at 1000 km from impact site. (Wave height above mean sea level is half this value). This was obtained from the energy of impact of the asteroid allowing for atmospheric dissipation and scaled from the results of experiments with nuclear explosives.

equation in modeling the propagation from the impact point to the shore. Dispersion is only important if the wave propagation distance is several thousand kilometers.

II. RUNUPS FROM LARGE IMPACTORS

The wavelengths of tsunami produced by larger asteroids are long enough that wave dispersion is not a problem. We can model these tsunami accurately using the shallow water (or long-wavelength) approximation. We initially used the SWAN code (Mader 1988) for these calculations. This for-

tran code has been tested extensively by comparing the runups predicted by the model against historical tsunami from earthquakes and landslides. M.P. Goda rewrote the SWAN code in the computer language C. The rewrite included the development of faster numerical algorithms and importation of an improved graphics package for displaying the tsunami runups. The code was tested against the original SWAN code to assure its accuracy. This new code will be ported to a massively parallel computer in the near future to allow runup calculations on a much finer grid than is practical with our current machines.

The simulation of the runups by large impactors allows us to find areas off the coast of Europe (and North America) that are particularly sensitive to tsunami. Later, we will investigate how sensitive these areas are to the multitude of many small impacts that occur between large impacts.

Figure 1 is not likely to be accurate for asteroids with radii much greater than 1 km because of the formation of a crater in the rock below the ocean and the reflection of some of the shock energy back into the ocean from the higher density rock below it. To simulate the effect of the impact of a large asteroid, we have taken as a test problem a crater 150 km across in the middle of the Atlantic Ocean. On land, craters this size would be produced by asteroids about 20 times smaller than the crater or about 7.5 km in diameter. For example the KT-impactor, which is estimated to have been 10 km in diameter, produced a crater about 200 km across in the Yucatan Penninsula. However, because of the lower density of the water and the likelihood that some of the shock energy is reflected back into the water from the ocean floor, we suspect that the ratio is more likely 30-to-one for a large impactor in water, so the asteroid responsible for our test crater would be about 5 km in diameter. An object at least this large impacts Earth every 10 million years. The location of the crater used in the numerical model is at 40° W and 35° N.

We previously discussed the effect of the tsunami from this impactor on the shores of North America (Hills and Mader 1997). It was found that the wave traveled all the way to the Appalachian Mountains in the upper two-thirds of the United States. Here we consider the effect of this hypothetical impact on Western Europe.

We first modeled the propagation of the tsunami produced by this crater from the impact point to the ocean off Europe using the New SWAN code, which is now called SWIM (Shallow Water Inundation Model), with the topographical ocean depth being determined by ETOPO5 (from US Defense
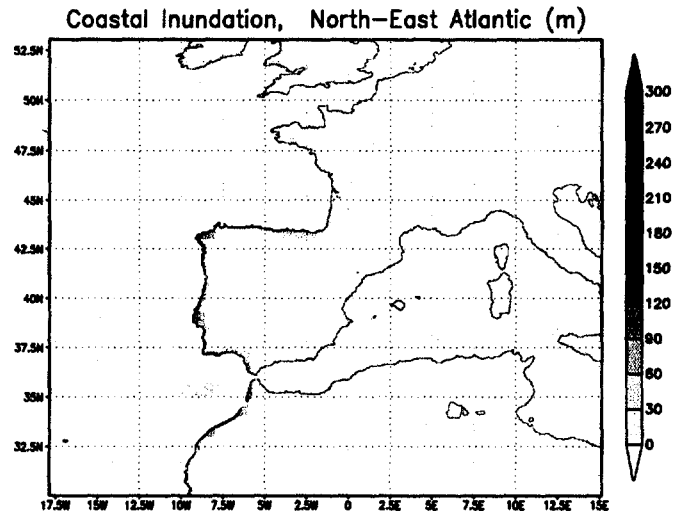
Coastal Inundation, North–East Atlantic (m)

Figure 2: Regions of Western Europe that had been inundated by the time the calculations had to be terminated. The grey scale shows the maximum depth of inundation above mean sea level reached at each location.

Mapping Agency). This gave a grid with a topographical resolution of 5 arc minutes. We found the height and wavelength of this wave before it came ashore in Europe. We then restarted the calculation on the part of Europe shown in Fig. 2. We used a piston on the western boundary of this grid that approximated the wavelength and amplitude of the wave found in the previous calculation. This handover reduced the tendency towards numerical instabilities at the free ocean surfaces at the corners of the numerical grid. The western boundary at 18 degrees longitude used a sinusoidal piston with an initial amplitude of 150 meters, a period of 903.51 seconds, a wavelength of 200 kilometers which corresponds to a deep water gravity wave speed of 221.35 m/s. After three strokes the piston decayed exponentially with an e-folding time of about one period. The remaining boundaries (where water is located) are linear continuous. No friction is used in the current runs. The code ran for 24000 model seconds (6.67 hours), which is sufficient time for all initial waves to interact with the coastlines. The code was then stopped due to numerical problems with waves at the continuous boundaries within the water.

Figures 3–6 show the extent of the flooding by the time the computations were stopped. The gray scale in the figures shows the maximum flood

depth attained at each location. The situation in Europe is much less serious than that in North America due to the extensive continental shelf protecting Northern Europe. This shelf reflects much of the tsunami energy back into the Atlantic. However, there is no significant continental shelf off the Iberian Peninsula, which causes it to suffer large tsunami runups. We see large surges inland in the vicinity of Lisbon, Portugal, Seville in southern Spain, and the Atlantic providences of France.
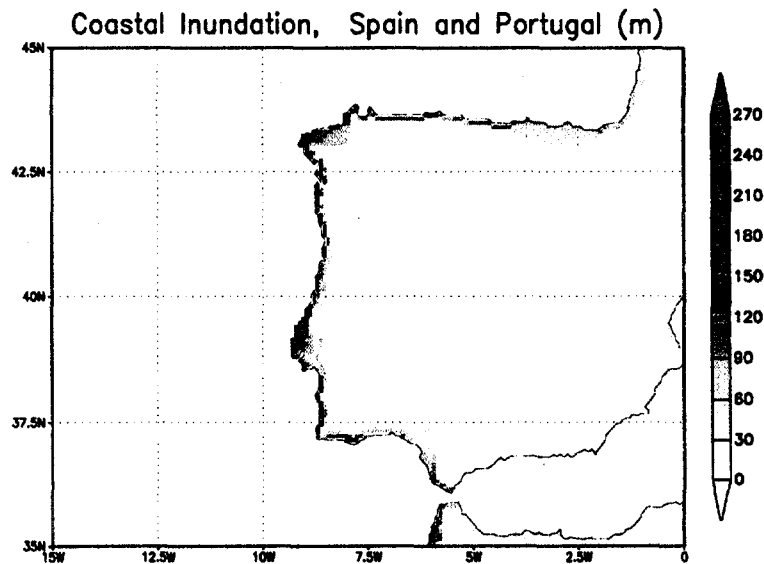
Figure 3: Same as Fig. 2 but with emphasis on Spain and Portugal.

Our computer simulations show inundations along the Iberian coast with depths of over 100 meters. The cliffs along the northern coast of the peninsula produce tsunami runups of about 300 meters. Deep inundations also occur along the Atlantic providences of France.

The wave enters the Straits of Gibraltar as a hydraulic bore. The width of the bore after it passes through the straits is comparable to that of the straits. Later it disperses laterally to produce tsunami in southern France and northern Morocco.

At the time we stopped the integration, Northern Europe was not as badly inundated as the Iberian Peninsula, at least in depth of inundation. This relief was largely due to much of the tsunami being reflected back into the Atlantic by the continental shelf. However, it may be a matter of indifference

to someone in Cork, Ireland to be inundated to a depth of a mere 20 meters as opposed to his brethren in Portugal being inundated by waves an order of magnitude higher!
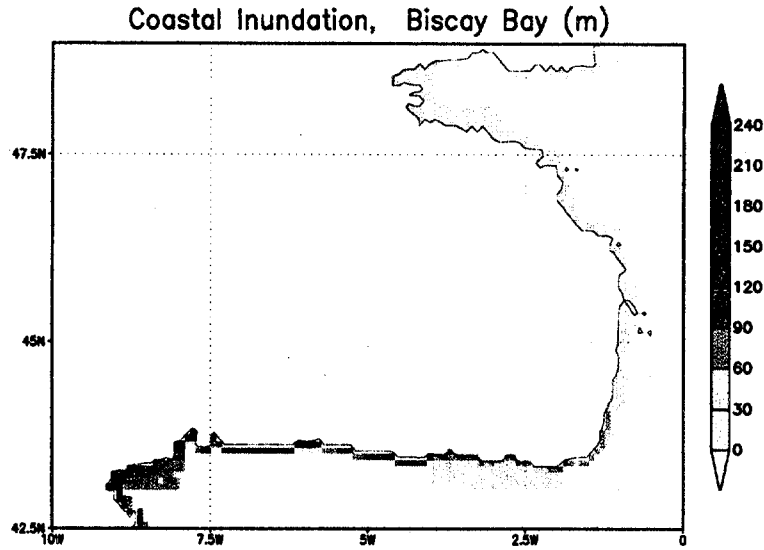
Figure 4: Same as Fig. 2 but with emphasis on Biscay Bay.
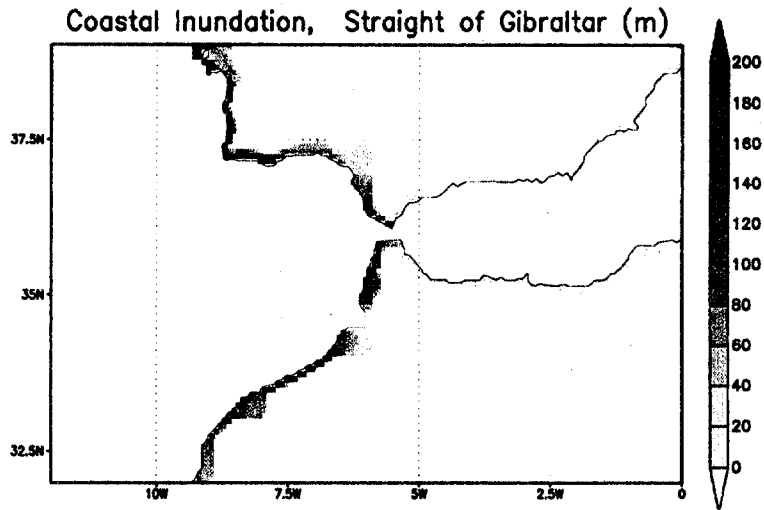
Figure 5: Same as Fig. 2 but with emphasis on the Straight of Gibraltar.

Coastal Inundation,   Southern Ireland and UK (m)
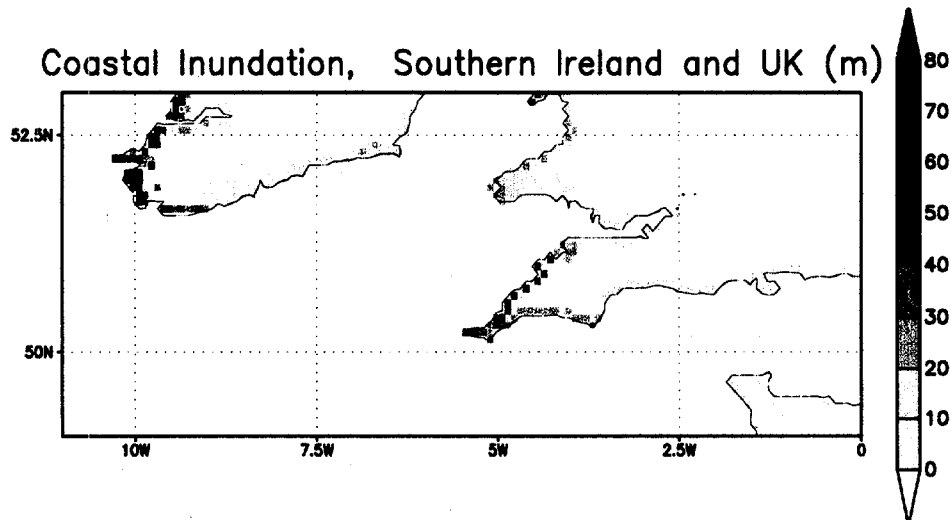
Figure 6: Same as Fig. 2 but with emphasis on southern regions of Ireland and the United Kingdom.

IV. REFERENCES

Glasstone, S. and Dolan, P.J. 1977, The Effects of Nuclear Weapons, third Ed. (U. S. Government Printing Office, Washington, DC).

Hills, J.G. and Goda, M.P. 1993, Astron. J. 105, 1114-1144, "The Fragmentation of Small Asteroids in the Atmosphere."

Hills, J.G. and Goda, M.P. 1998, Planet. Space Sci. 46, No. 2/3, 219-229, "Damage from the Impacts of Small Asteroids".

Hills, J.G. and Mader, C.L., 1997, in Near-Earth Objects, Annals of the New York Academy of Sciences, 822, 381-394 "Tsunami Produced by Impacts of Small Asteroids".

Mader, C.L. 1988, Numerical Modeling of Water Waves (University of California Press, Berkeley).

ASTEROID TSUNAMI INUNDATION OF JAPAN

Charles L. Mader

Mader Consulting Co.

Honolulu, HI., U.S.A.

ABSTRACT

A study of the tsunami wave inundation to be expected from an asteroid impact with the ocean is in progress. The recent Shoemaker-Levy-9 asteroid impact with Jupiter or the Eltanin asteroid that impacted the Southern Pacific ocean 2.16 million years ago are typical of the type of event being studied.

The asteroid generated cavity modeled was 120 kilometers in diameter and 5 kilometers deep which approximates the cavity that was generated by the Eltanin asteroid or would have been generated by the Shoemaker-Levy-9 asteroid.

The modeling was performed using the *SWAN* code which solves the nonlinear long wave equations. The tsunami generation, propagation, and inundation was modeled using a 2.0 minute Mercator grid of 600 by 579 cells.

The asteroid tsunami wave inundated Tokyo to 70 meters and parts of the Japan coast to 300 meters.

INTRODUCTION

The impact site of the Eltanin asteroid in the Southern Pacific Ocean at 57.78 S, 90.79 W has been described by Gersonde, Kyte, Bleil, Diekmann, Flores, Gohl, Grahl, Hagen, Kuhn, Sierro, Volker, Abermann and Bostwick in Reference 1. The event took place about 2.16 million years ago and could have been caused by an asteroid about 4 kilometers in size moving 20 kilometers/second.

If such an asteroid struck the ocean near Japan it would generate a tsunami wave over 100 meters high and with a period of over 1000 seconds in the deep ocean outside the coast of Japan. A Shoemaker-Levy-9 asteroid would generate a similar tsunami wave.

MODELING

The asteroid was assumed to interact with the ocean about 360 kilometers east of Tokyo at 35.3N and 143.3 E. The cavity generated by the asteroid was 120 kilometers in diameter and 5 kilometers deep or to the ocean floor which ever was smaller.

The modeling was performed using the *SWAN* non-linear shallow water code which includes Coriolis and frictional effects. The *SWAN* code is described in Reference 2. The calculations were performed on 233 Mhz Pentium personal computers with 48 megabytes of memory.

The asteroid tsunami inundation of Hawaii was modeled using the *SWAN* code as described in Reference 3. The code was also used to study an asteroid generated tsunami between Hawaii and Australia as described in Reference 4.

The Japan topography was generated from the 2 minute Mercator Global Marine Gravity topography of the earth of Sandwell and Smith of the Scripps Institute of Oceanography and described in Reference 5. The grid was 600 by 579 cells with the left hand corner at 31 N, 131 E. The grid extended from 31 N to 46 N and from 131 E to 151 E. The time step was 3 seconds.

The calculated wave amplitudes at various locations as a function of time are shown in Figure 1. The axis units are time in seconds and height in meters. Location 1 was 11 meters above sea level, location 4 was in 206 meter deep water, location 5 in 5870 meters, and location 6 in 5888 meters.

The wave contours are shown in Figure 2 at various times. The contour interval is 50 meters and the units of the X and Y axis are 10 kilometers.

As shown in References 2, 3, and 4 the run-up amplification is from 2 to 3 times the deep water wave amplitude.

The inundation of the Tokyo region is shown in Figure 3. All of Tokyo below 50 meters is inundated and parts of the coast are flooded to 300 meters.

Computer generated animations of these calculations are available from the author.

REFERENCES

1. R. Gersonde, F. T. Kyte, U. Bleil, B. Diekmann, J. A. Flores, K. Gohl, G. Grahl, R. Hagen, G. Kuhn, F. J. Sierro, D. Volker, A. Abelmann, and J. A. Bostwick *Geological Record and Reconstruction of the Late Pliocene Impact of the Eltanin Asteroid in the Southern Ocean*, Nature, **390**, 357-363, November 27, 1997.
2. Charles L. Mader *Numerical Modeling of Water Waves,* University of California Press, Berkeley, California (1988).
3. Charles L. Mader *Asteroid Tsunami Inundation of Hawaii*, Science of Tsunami Hazards, **14**, 85-88 (1996).
4. Anthony T. Jones and Charles L. Mader *Modeling of Tsunami Propagation Directed at Wave Erosion on Southeastern Australian Coast 104,000 Years ago*, Science of Tsunami Hazards, **13**, 45-52 (1995).
5. W. H. F. Smith and D. T. Sandwell, *Global Seafloor Topography from Satellite Altimetry and Ship Depth Soundings,* Science, April 7, 1997.
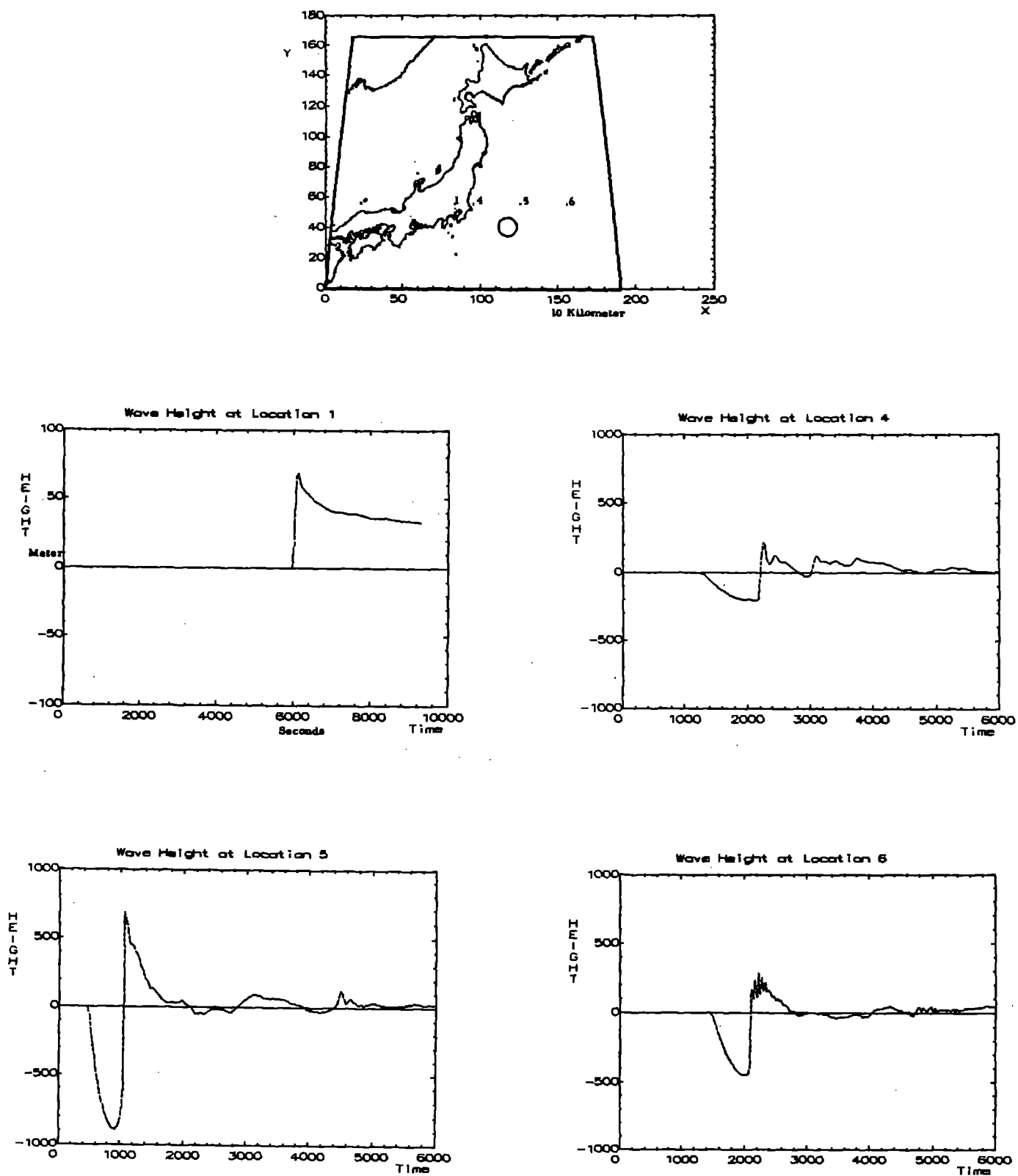
Figure 1. The calculated wave amplitudes in meters at various locations as
a function of time in seconds. Location 1 was 11 meters above sea
level, location 4 was in 206 meter deep water, location 5 in 5870
meters, and location 6 in 5888 meters.

O. min, INC= 50.

5. min, INC= 50.
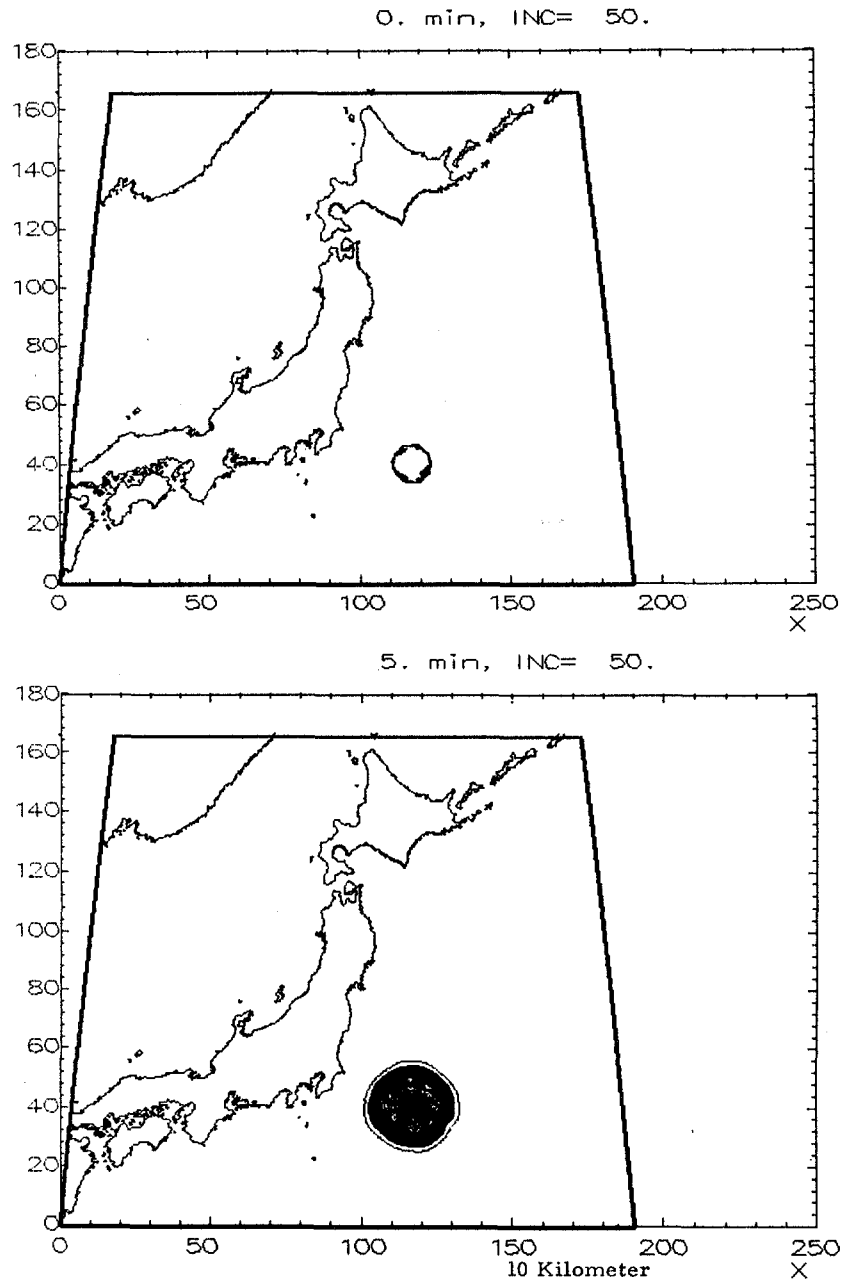
10 Kilometer

Figure 2. The wave contours generated by a 120 kilometer diameter cavity
are shown at various times. The contour interval is 50 meters and
the units of the X and Y axis are 10 kilometers.

20. min, INC= 50.
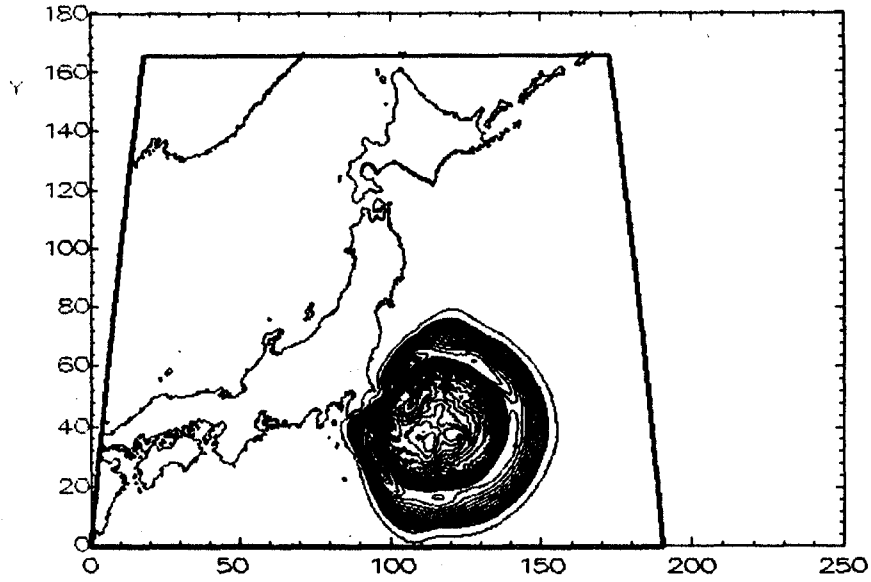
45. min, INC= 50.
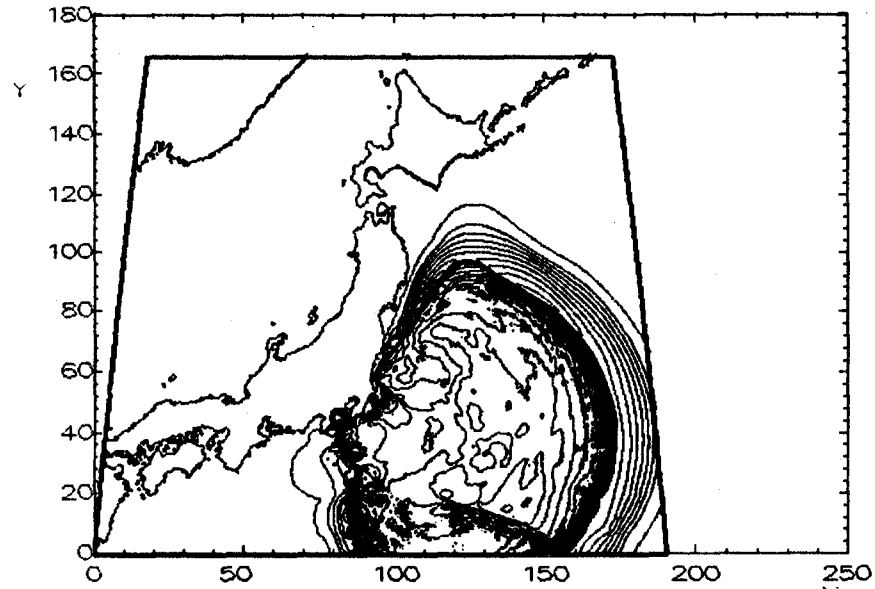
80. min, INC= 50.
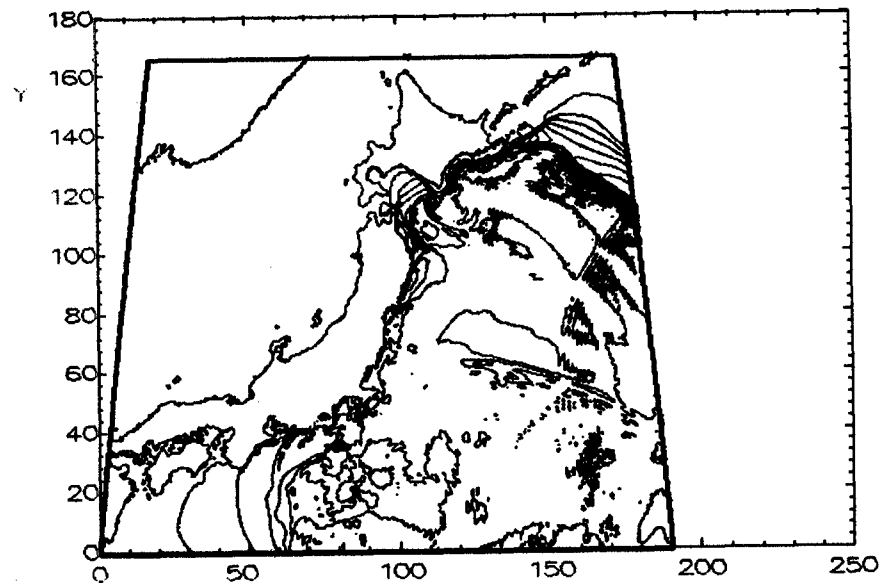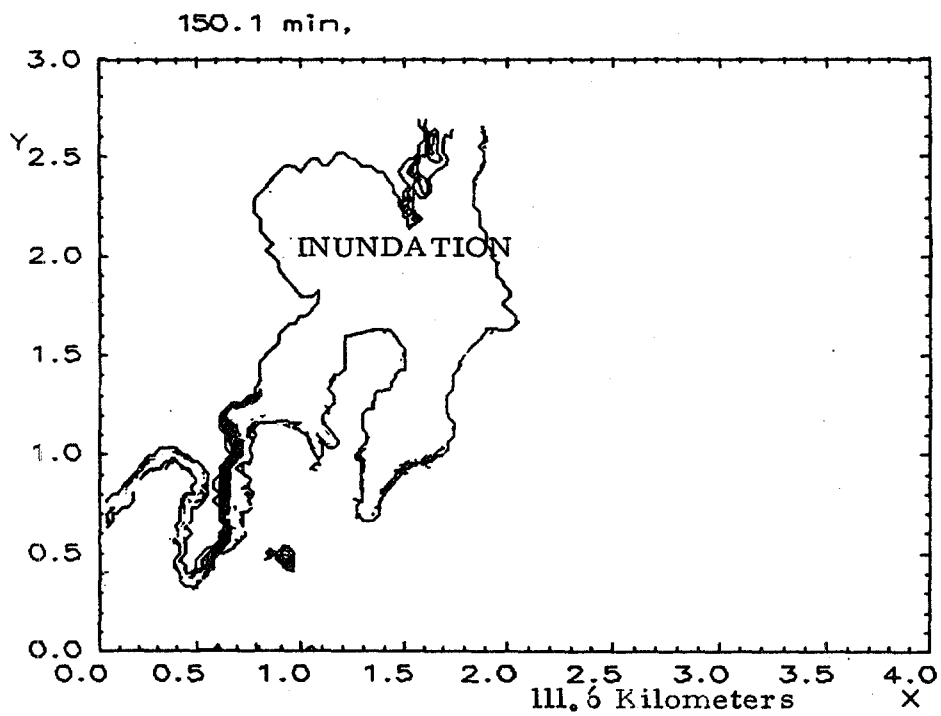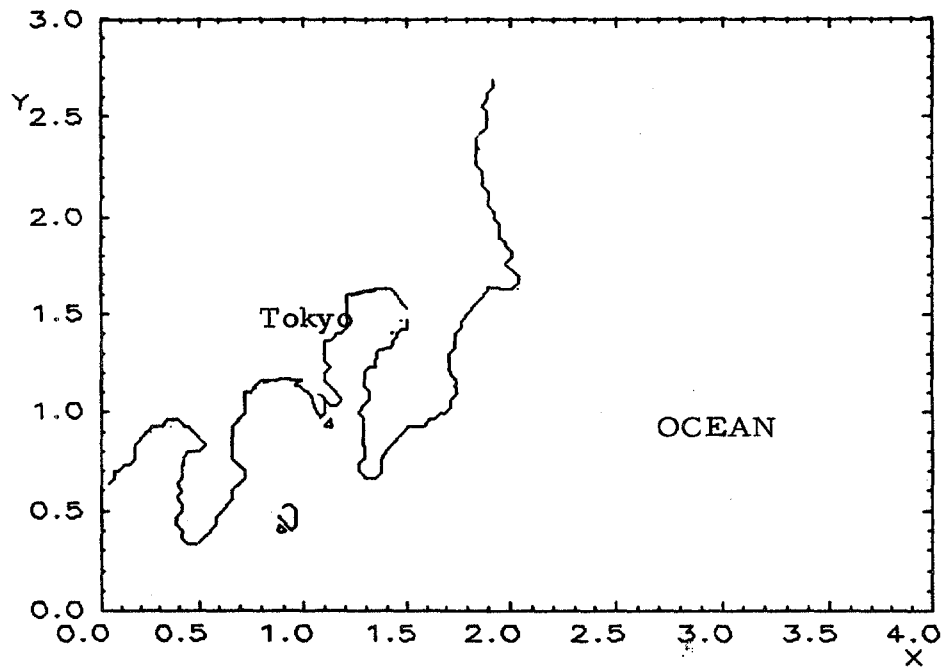
Figure 3. The inundation of the Tokyo region is shown. All of Tokyo below
50 meters is inundated and parts of the coast are flooded to 300
meters.

MODELING THE ELTANIN ASTEROID TSUNAMI

Charles L. Mader

Mader Consulting Co.

Honolulu, HI., U.S.A.

ABSTRACT

The generation and propagation of a tsunami off the coast of Chile by the Eltanin asteroid about 2.16 million years ago was modeled. The tsunami wave was generated from an ocean cavity 80 kilometers wide, 150 kilometers long and 5 kilometers deep located at 57.78 S, 90.79 W which approximates the cavity that the Eltanin asteroid could have generated.

The modeling was performed using the *SWAN* code which solves the nonlinear long wave equations.

The tsunami generation and propagation was modeled using a 20.0 minute ETOPO grid for the Pacific ocean.

The tsunami wave had a period of 1000 to 2000 seconds and maximum amplitudes in deep water of 80 meters off the South Coast of Chile, 65 meters in the Drake Passage, 40 meters off New Zealand, 28 meters off Hawaii, 20 meters off the California coast, 30 meters in the Gulf of Alaska, and 8 meters off Japan.

If a larger asteroid similar to the KT event 65 million year ago struck at the Eltanin impact site, the wave heights would be 130 meters off Hawaii, 40 meters off the California coast, and 60 meters off Japan.

INTRODUCTION

The impact site of the Eltanin asteroid in the Southern Ocean at 57.78 S, 90.79 W has been described by Gersonde, Kyte, Bleil, Diekmann, Flores, Gohl, Grahl, Hagen, Kuhn, Sierro, Volker, Abermann and Bostwick in Reference 1. The event took place about 2.16 million years ago and could have been caused by an asteroid about 4 kilometers in size moving 20 kilometers/second. The asteroid did not make a cavity in the ocean floor nor did it result in any extinctions. Such an asteroid would be expected to generate a cavity in the ocean of approximately 100 to 150 kilometer diameter. Since it did not generate a cavity in the ocean floor its impact angle was probably 45 degrees or less.

MODELING

The generation and propagation of the tsunami wave generated by the Eltanin Asteriod was modeled using a 20.0 minute grid of the Pacific basin topography. The modeling was performed using the *SWAN* non-linear shallow water code which includes Coriolis and frictional effects. The *SWAN* code is described in Reference 2. The calculations were performed on 160 Mhz Pentium personal computers with 16 megabytes of memory. The 5 minute topography from the NOAA ETOPO 5 minute grid of the earth was used to generate the 20 minute grid. The grid was 600 by 450 cells and the time step was 30 seconds. The eastern boundary of the calculation had a small diurnal tide to keep the eastern boundary numerically stable.

The asteroid tsunami inundation of Hawaii was modeled using the *SWAN* code as described in Reference 3. The code was also used to study an asteroid generated tsunami between Hawaii and Australia as described in Reference 4.

The initial cavity was 4 by 4 cells or 150 by 80 kilometers which has the volume of a 120 kilometer diameter cavity. The depth of the cavity was to the ocean floor which varied from 4951 to 5048 meters.

The calculated maximum wave amplitudes at various locations shown in Figure 1 are given in Table 1.

With decreasing periods and wavelengths, the discrepancy between shallow water and Navier Stokes waves formed from initial sea displacement increases as shown in Reference 5. The amplitudes in Table 1 are upper limit values and as much as twice too large at long distances of run. As shown in References 2, 3, and 4 the run-up amplification is from 2 to 3 times the deep water wave amplitude. So the calculated amplitudes in the North Pacific are close to the expected inundation limits.

If a large asteroid similar to the KT asteroid struck the Eltanin impact site, the cavity would have been about 500 kilometers wide and would generate waves with the amplitudes shown in Table 2. The travel time chart for such a wave is shown in Figure 2.

In reference 6, page 163, Duncan Steel states that the comet impacts on Jupiter similar to the one that occured in July 1994 were observed in 1883, 1928, 1939 and 1948 or five collision events per century. Jupiter is likely to be struck about 1000 times as often as the earth which implies that the earth will be hit every 20,000 years by an asteroid that could generate a tsunami that was a hazard throughout the entire Atlantic or Pacific basin. However, as discussed in references 6 and 7 when large asteroids next impact the planet, tsunamis will probably be the least of the problems for life on our earth.

REFERENCES

1. R. Gersonde, F. T. Kyte, U. Bleil, B. Diekmann, J. A. Flores, K. Gohl, G. Grahl, R. Hagen, G. Kuhn, F. J. Sierro, D. Volker, A. Abelmann, and J. A. Bostwick *Geological Record and Reconstruction of the Late Pliocene Impact of the Eltanin Asteroid in the Southern Ocean*, Nature, **390**, 357-363, November 27, 1997.
2. Charles L. Mader *Numerical Modeling of Water Waves*, University of California Press, Berkeley, California (1988).
3. Charles L. Mader *Asteroid Tsunami Inundation of Hawaii*, Science of Tsunami Hazards, **14**, 85-88 (1996).
4. Anthony T. Jones and Charles L. Mader *Modeling of Tsunami Propagation Directed at Wave Erosion on Southeastern Australian Coast 104,000 Years ago*, Science of Tsunami Hazards, **13**, 45-52 (1995).
5. Charles L. Mader *Numerical Tsunami Propagation Study III*, Science of Tsunami Hazards, **11**, 93-108 (1993).
6. Gerrit L. Verschurr, *Impact-The Threat of Comets and Asteroids*, Oxford University Press (1996).
7. Duncan Steele, *Rogue Asteroids and Doomsday Comets*, John Wiley and Sons (1995).

Figure 2. The tsunami travel time hourly profiles

Figure 1. The locations in Table 1.

TABLE 1
CALCULATED DEEP WATER WAVE HEIGHTS
FOR ELTANIN TSUNAMI

No	Depth Meters	Location	Maximum Amplitude Meters	Minimum Amplitude Meters
1	2921	Drake Passage	+65	-65
2	4057	San Paulo, Brazil	+5	-10
3	3115	South Chile	+80	-100
4	4787	Lima, Peru	+25	-35
5	5066	East of New Zealand	+40	-40
6	4321	Hawaii	+28	-18
7	3556	California	+20	-20
1 A	3703	Gulf of Alaska	+30	-30
2 A	5989	Japan	+8	-8
3 A	3001	New Zealand	+40	-30
4 A	4685	Australia	+8	-8
5 A	4869	Near Source	+160	-200
6 A	4592	Near Source	+130	-140
7 A	4283	Near Source	+110	-110

TABLE 2
CALCULATED DEEP WATER WAVE HEIGHTS
FOR KT ASTEROID TSUNAMI
IMPACTING AT ELTANIN SITE

No	Depth Meters	Location	Maximum Amplitude Meters	Minimum Amplitude Meters
1	2921	Drake Passage	+220	-240
1A	3703	Gulf of Alaska	+60	-260
2A	5989	Japan	+60	-45
4	4787	Lima, Peru	+100	-400
3A	3001	New Zealand	+200	-160
6	4321	Hawaii	+130	-150
7	3556	California	+40	-170

MODELING ASTERIOD IMPACT AND TSUNAMI

David A. Crawford
Sandia National Laboratories
Albuquerque, NM 87185-0820, U.S.A.

Charles L. Mader
Mader Consulting Co.
Honolulu, HI 96825-2860, U.S.A.

ABSTRACT

A study of the interaction of a typical stony asteroid (density of 3.32 g/cc and velocity of 20 km/sec) with the atmosphere, and a 5 km deep ocean with a basalt bottom has been modeled using the CTH computer code for multidimensional, multi-material, large deformation, strong shock wave physics. Two dimensional axial symmetric calculations were performed for up one minute of real time. This was adequate to follow the ocean cavity formation until maximum cavity size for 250, 500, and 1000 meter diameter asteroids. The maximum hemispherical cavity size was 2500, and 5000 in radius for the 250 and 500 meter asteroid. The maximum cavity size was a 5 km deep, 10 km radius cylinder for the 1 km diameter asteroid.

The collapse of the cavities, the resulting tsunami waves and the propagation for up to 150 km was modeled using the the *ZUNI* code which solves the incompressible Navier-Stokes equations.

A 250 meter asteroid would result in less than a a 10 meter high tsunami after 60 km of travel, a 500 meter asteroid would result in a 100 meter high wave after 30 km of travel and in a 10 meter high tsunami after 200 km of travel. The tsunami generated by a 1 km diameter asteroid would run 80 km before the tsunami wave amplitude was less than 100 meters and 500 km before it was less than 10 meters. The tsunami period, wavelength and velocity increases with run distance while the amplitude decreases. The tsunami wave amplitudes and velocities are less than the shallow water wave values.

ASTEROID TSUNAMIS

The Sandia CTH shock physics code was used in 1994 by Crawford and Boslough to accurately simulate what happened when comet Shoemaker-Levy 9 plunged into Jupiter's atmosphere as described in references 1 and 2. Months later, the world's astromers watched the Sandia predicted event unfold in real life through the Hubble space telescope.

The CTH code was used to model a three-dimensional 120 square mile space of the New York City metropolitan area, the air above, and the water and earth below using 100 million cells. An asteroid 1.4 kilometers in diameter struck the ocean at a 15 degree angle 25 miles south of Brooklyn, New York. The results of the calculations are shown in reference 3. An impact plume containing superheated water, earth and other debris blanketed major portions of Long Island. The calculation required 18 hours on the U. S. Department of Energy's ASCI teraflops computer to run to 8.4 seconds after impact.

Tsunami waves generated by earthquakes have typically had a maximum deep ocean amplitude of 10 meters and periods of 500 to 2000 seconds. Tsunami waves with amplitudes of approximately 100 meters are referred to as mega-tsunamis and may be generated by landslides such as the 105 Ka Lanai event described in reference 4 or by asteroid impact with the ocean described in reference 5. The landslide tsunamis have shorter periods and thus the tsunami wave amplitude is not maintained as the wave travels from the source. Large asteroid generated tsunami waves have long periods and waves with large amplitudes that can propagate across an ocean basin.

MODELING THE ASTEROID TSUNAMI

A study of the interaction of a typical stony asteroid (density of 3.32 g/cc and velocity of 20 km/sec) with a 5 km deep ocean with a basalt bottom has been modeled using the CTH computer code for multidimensional, multi-material, large deformation, strong shock wave physics described in reference 6. Two dimensional axial symmetric calculations were performed using a 5, 50 and 100 meter grids for up to one minute of real time. This was adequate to follow the ocean cavity formation until maximum cavity size for 250, 500, and 1000 meter diameter asteroids. The maximum hemispherical cavity size was 2500, and 5000 in radius for the 250 and 500 meter asteroid. The maximum cavity size was a 5 km deep, 10 km radius cylinder for the 1 km diameter asteroid. The interface profiles at various times are shown in Figure 1 for the 500 meter diameter asteroid. The maximum cavity occurs at 21 seconds. The profile at maximum transient cavity size is shown in Figure 2 for the 250 meter diameter asteroid, and in Figure 3 for the 1000 meter diameter asteroid.

The collapse of the cavities, the resulting tsunami waves and the propagation for up to 150 km was modeled. The modeling was performed using the ZUNI incompressible Navier-Stokes code. The ZUNI code is described in reference 7. The calculations were performed on 230 Mhz Pentium personal computers.

A summary of the tsunami wave heights at various distances of run in a 5000 meter deep ocean are shown in Table 1. A 250 meter asteroid would result in less than a a 10 meter high tsunami after 60 km of travel, a 500 meter asteroid would result in a 100 meter high wave after 30 km of travel and in a 10 meter high tsunami after 200 km of travel, a 1 km diameter asteroid would run 80 km before the tsunami wave amplitude was less than

100 meters and 500 km before it was less than 10 meters. The tsunami period, wavelength and velocity increases with run distance while the amplitude decreases. The tsunami wave amplitudes and velocities are less than the shallow water wave values shown in Table 2. As described in reference 7, the shallow water cavity collapses from the side while the Navier-Stokes cavity collapses primarily from the bottom. The resulting wave amplitude after collapse at the initial cavity radius for the Navier-Stokes cavity is less than half of that for the shallow water cavity.

DISCUSSION

Some of the estimates in the technical literature of tsunami wave heights generated by asteroids are described by Verschuur in reference 8, Steel in reference 9, and Lewis in reference 10. A one kilometer stony asteroid traveling 20 kilometers/sec has been estimated to generate a 200 meter high tsunami after 1000 kilometers of run. As shown in Table 1, the tsunami wave amplitude would be about 6 meters.

A 500 meter stony asteroid has been estimated to generate a 50 to 100 meter high tsunami after 1000 kilometers of run. The wave amplitude from Table 1 would be less than 2 meters. If one assumes that the tsunami wave travels 1000 kilometers as a shallow water wave, the geometrical aspect alone would lower the wave amplitude to about 5 meters. The tsunami wave period after the wave has run 10 kilometers is about 3 minutes and the wave length is about 30 kilometers. In a 5 kilometer ocean this wave is not a shallow water wave.

Most tsunami waves that have been observed after traveling across the ocean have periods longer than 10 minutes. As shown in reference 11, this is because short wave length tsunamis are so dispersive that as they propagate long distances, their amplitude decreases by an order of magnitude.

The 500 meter diameter stony asteroid generated tsunami has been attributed in the press and technical literature as presenting a hazard throughout the entire Atlantic or Pacific basin regardless of where it impacts the ocean. It would actually require an asteroid with a diameter greater than 2 kilometers.

The modeling of the cavity generated by the asteroid impact and the use of the maximum cavity size to calculate tsunami wave amplitudes furnishes wave amplitudes as a function of distance of run that are uncertain by at least a factor of two. Future modeling of asteroid generated tsunami waves need to be performed using numerical models that will follow the compressible to incompressible fluid dynamics as a single continuous problem. The effect of asteroid velocity, density, composition and the state properties of the ocean floor need to be evaluated.

Acknowledgments
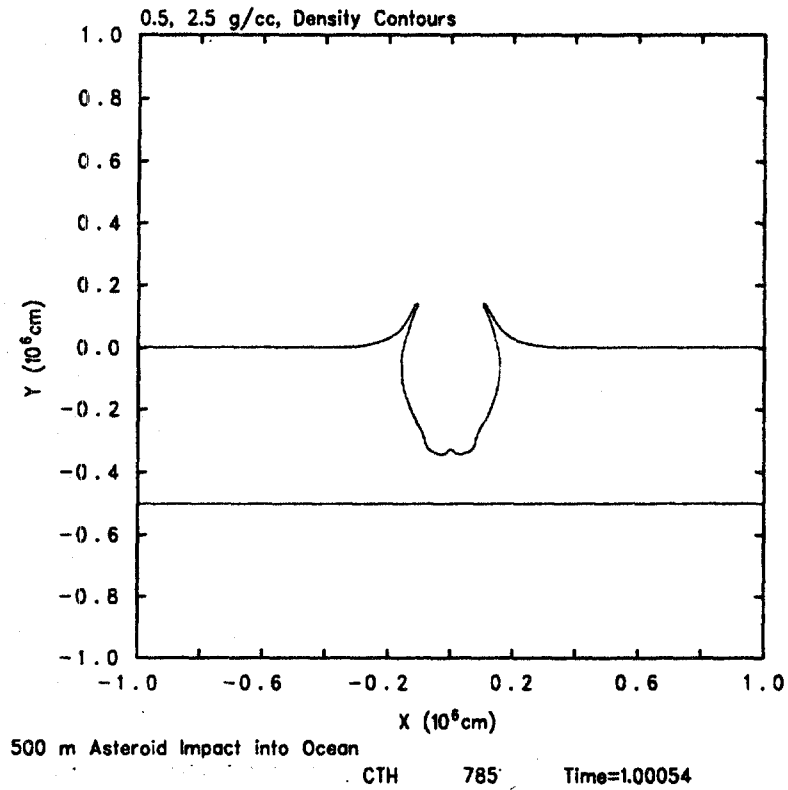
Figure 1. A 500 meter diameter, dunite asteroid moving 20 kilometers/second impacting 5000 meters of water and a basalt ocean floor. The maximum cavity occurs at 21 seconds.

0.5, 2.5 g/cc, Density Contours

Y (10^5cm)

X (10^5cm)

500 m Asteroid Impact into Ocean

CTH   3124   Time=1.00024x10^1

0.5, 2.5 g/cc, Density Contours

Y (10^5cm)

X (10^5cm)

500 m Asteroid Impact into Ocean

CTH   5823   Time=2.10024x10^1

0.5, 2.5 g/cc, Density Contours

Y (10^8cm)

X (10^8cm)

500 m Asteroid Impact Into Ocean

CTH   6801   Time=2.50025x10^1

0.5, 2.5 g/cc, Density Contours

Y (10^8cm)

X (10^8cm)

500 m Asteroid Impact Into Ocean

CTH   8024   Time=3.00015x10^1

0.5, 2.5 g/cc, Density Contours

250 m Asteroid Impact Into Ocean

CTH   6937   Time=1.350×10¹
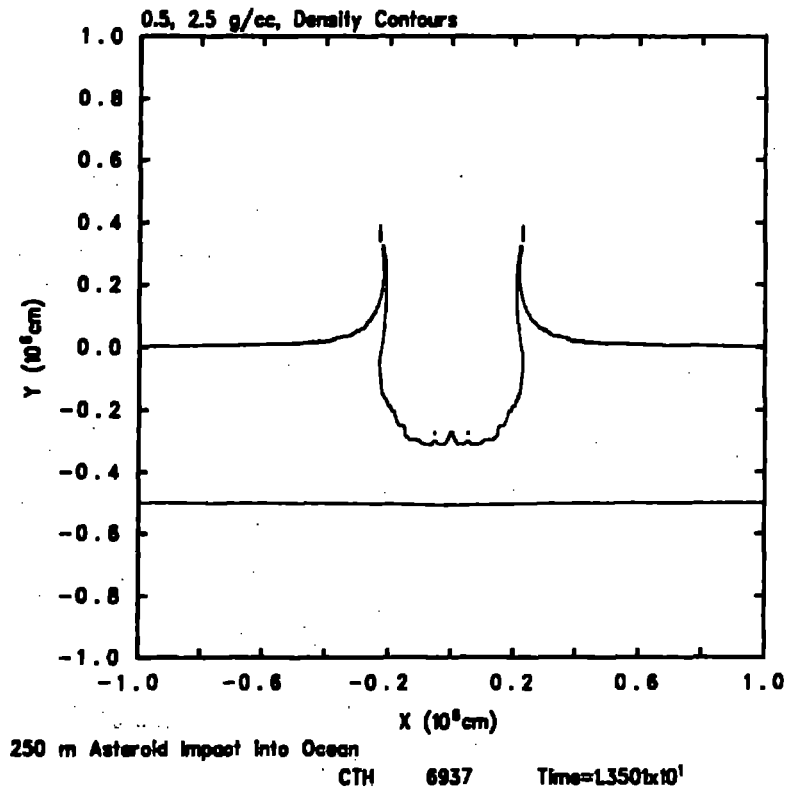
Figure 2. The maximum ocean cavity generated by a 250 meter diameter, 3.32 g/cc asteroid moving 20 kilometers/second impacting 5000 meters of water and a basalt ocean floor. The maximum cavity occurs at 13 seconds.

1000 m Asteroid Impact Into Ocean

CTH   4204   Time=3.40076×10¹
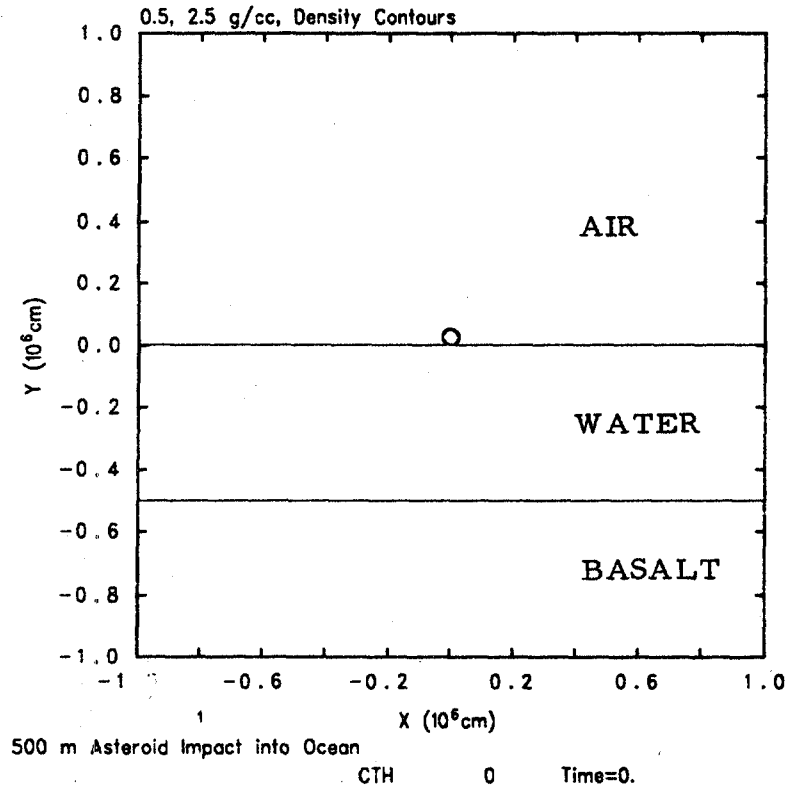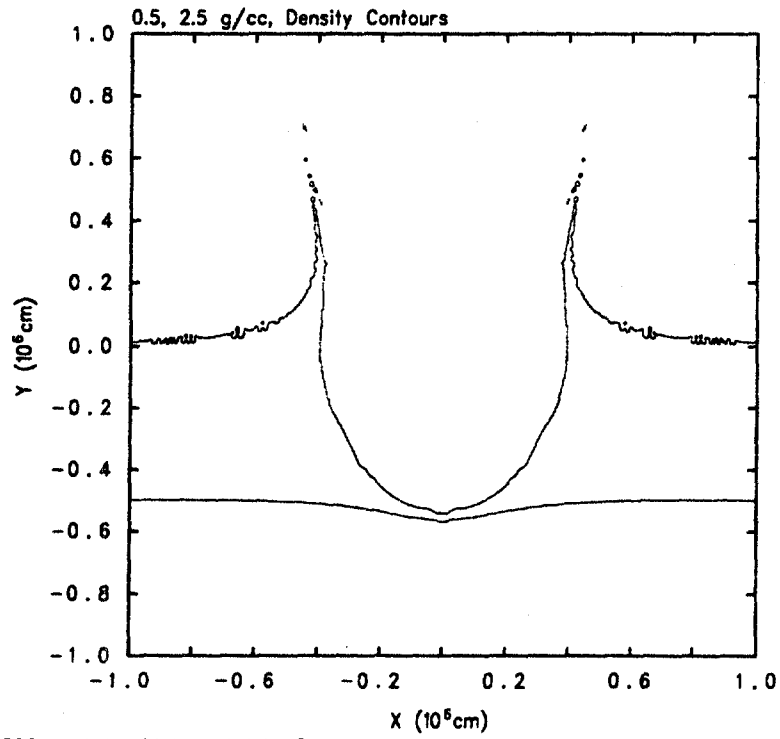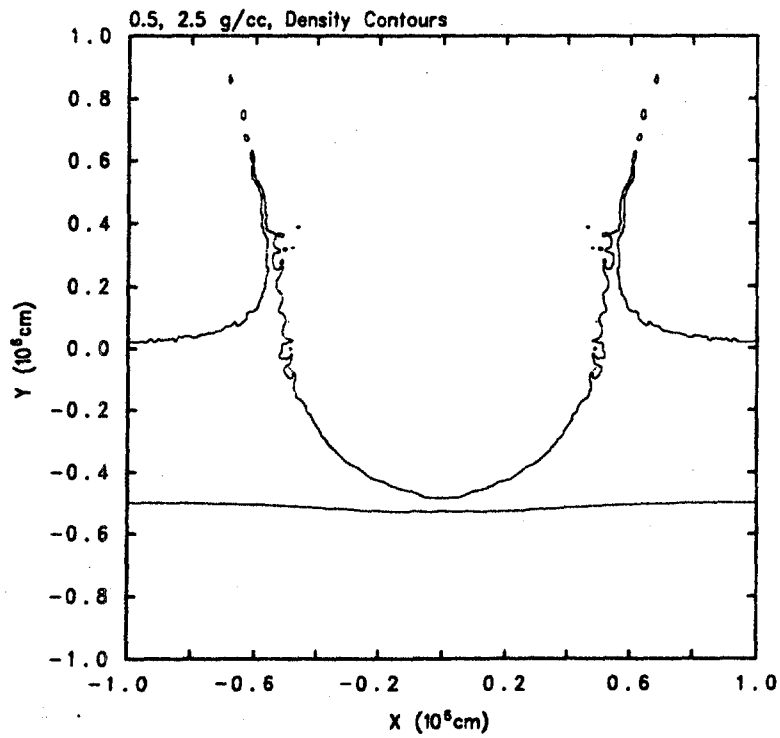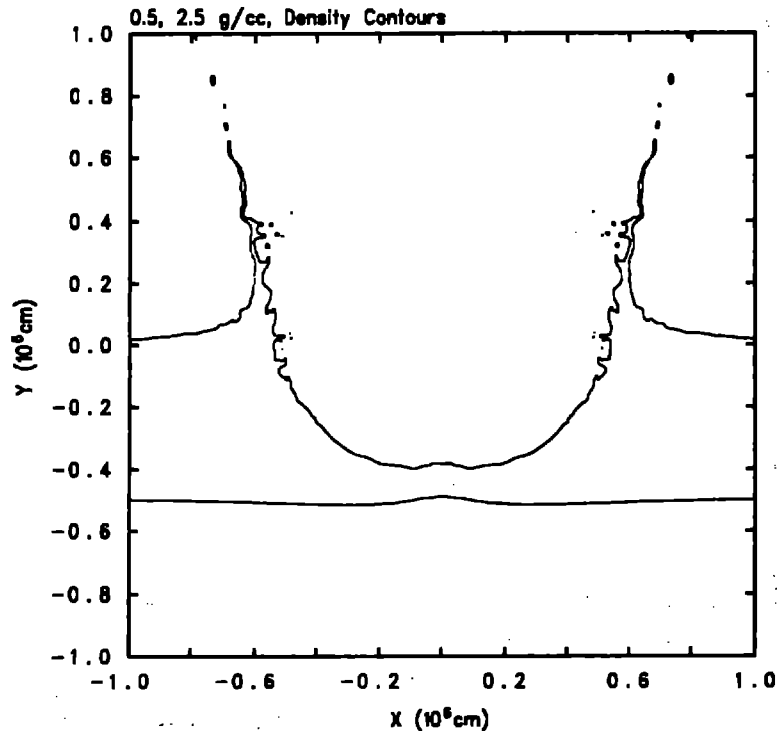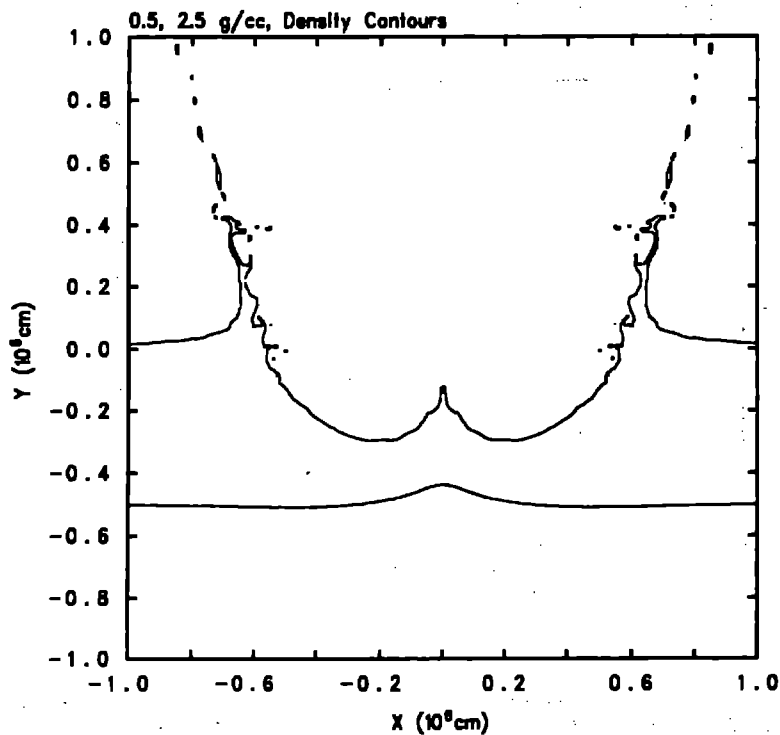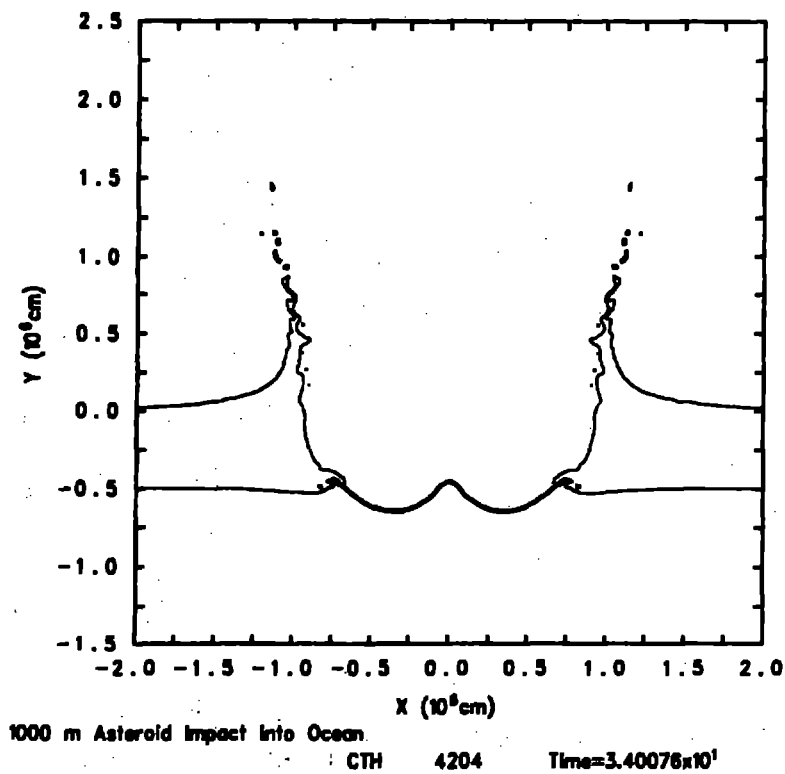
Figure 3. The maximum ocean cavity generated by a 1000 meter diameter, 3.32 g/cc asteroid moving 20 kilometers/second and impacting 5000 meters of water and a basalt ocean floor. The maximum cavity occurs at 34 seconds.

Table 1.
Asteroid Tsunami Wave Heights

| Asteroid Dia (m) | 250. | 500. | 1,000. | | |
Water Cavity[a] Radius (m) (Ro)	2,500.	5,000.	10,000.	20,000.	30,000.
1.0 km	800.	2800.	5000.	7500.	7900.
2.5 km	300.	1300.		4800.	5500.
5.0 km	150.	600.	1600.	3000.	3800.
10.0 km	72.	350.	900.	2000.	2400.
15.0 km	50.	220.	640.	1600.	2100.
20.0 km	34.	160.	460.	1250.	1700.
25.0 km	28.	120.	360.	1100.	1400.
30.0 km	22.	100.	300.	880.	1200.
40.0 km	16.	70.	220.	680.	900.
45.0 km	14.	62.	190.	600.	810.
50.0 km	12.	55.	170.	525.	720.
60.0 km	10.	43.	135.	425.	600.
70.0 km	8.	38.	110.	350.	510.
100. km		22.	70.	230.	360.
150. km		14.	40.	150.	
H(Ro/R)	EXTRAPO	LATED			
500. km			12.	50.	83.
1000. km			6.	26.	36.
H(Ro/R)	300.	600.	900.	1250.	1200.

	Values[b]	at	R/Ro=4	
Velocity (m/s)	166.	166.	190.	210.
Wave Length	24 km	32 km	56 km	90 km
Period	2.5 min	3 min	5 min	7 min

[a] CTH Asteroid Model - 3.32 g/cc Dunite, 20 km/sec,
 In 5 km Deep Ocean, Basalt Ocean Floor
[b] Tsunami period, wavelength, and velocity increases with run.

Table 2.

Shallow Water Asteroid Tsunami Wave Heights

Asteroid Dia (m)	250.	500.	1,000.
Water Cavity[a] Radius (m) (Ro)	2,500.	5,000.	10,000.
1.0 km			
2.5 km	725.		
5.0 km	550.	1100.	
7.5 km	360.		
9.0 km	300.		
10.0 km	(250.)	560.	1800.
15.0 km		360.	1700.
16.0 km			1500.
17.0 km			1300.
20.0 km	(125.)	250.	
25.0 km	(100.)	(220.)	(800.)
50.0 km	(50.)	(110.)	
75.0 km	(33.)	(73.)	
100. km	(10.)	(55.)	(200.)
150. km		(37.)	(133.)
500. km		(11.)	(40.)
1000. km		(6.)	(20.)
H(Ro/R)	1000.	1100.	2000.
Velocity (m/s)	221.	221.	221.
Wave Length	9 km	17 km	40 km
Period	40 sec	100 sec	180 sec

[a] CTH Asteroid Model - 3.32 g/cc Dunite, 20 km/sec,
In 5 km Deep Ocean, Basalt Ocean Floor
Values in Parenthesis are Calculated from H(Ro/R)

REFERENCES

1. D. A. Crawford, M. B. Boslough, T. C. Trucano and A. C. Robinson, "The Impact of Comet Shoemaker-Levy 9 on Jupiter," Shock Waves, Vol 4, pages 47-50 (1994).
2. M. B. Boslough, D. A. Crawford, A. C. Robinson, and T. G. Trucano, "Watching for Fireballs on Jupiter," EOS, Transactions, American Geophysical Union, Vol 75, pages 305-307 (1994).
3. Gerrit L. Vershurr *Impact Hazards*, Sky and Telescope, June 1998, pages 27-34.
4. Carl Johnson and Charles L. Mader, "Modeling the 105 Ka Lanai Tsunami", Science of Tsunami Hazards, Vol 11, pages 33-38 (1994).
5. Anthony T. Jones and Charles L. Mader, "Modeling of Tsunami Propagation Directed at Wave Erosion on Southeastern Australian Coast 104,000 Years Ago," Science of Tsunami Hazards, Vol 13, pages 45-52 (1995).
6. J. M. McGlaun and S. L. Thompson, "CTH: A Three-Dimensional Shock Wave Physics Code," International Journal of Impact Engineering, Vol 10, pages 351-360 (1990).
7. Charles L. Mader *Numerical Modeling of Water Waves*, University of California Press, Berkeley, California (1988).
8. Gerrit L. Verschurr, *Impact-The Threat of Comets and Asteroids*, Oxford University Press, page 153 (1996).
9. Duncan Steele, *Rogue Asteroids and Doomsday Comets*, John Wiley and Sons, page 40 (1995).
10. John S. Lewis, *Rain of Iron and Ice*, Addison-Wesley Publishing Co., page 150 (1996).
11. Charles L. Mader, Dennis W. Moore, and George F. Carrier, "Numerical Tsunami Propagation Study - III", Journal of Tsunami Hazards, pages 93-106 (1993).

POTENTIAL FOR LANDSLIDE-GENERATED TSUNAMIS IN HAWAII

Patricia A. Lockridge
National Geophysical Data Center
325 Broadway, Boulder, CO 80303-3328 U.S.A.

ABSTRACT

Very large landslides off the shores of Hawaii have probably generated gigantic tsunamis in the past. Additional landslides of this type may again generate immense tsunamis that will inundate large portions of the islands. The mechanism(s) for tsunami generation from landslides is discussed. Several historical landslide-generated tsunami events are cited. The special case of landslides from volcanic edifices is examined and historical evidence cited.

The mechanisms of island building and erosion in Hawaii are reviewed. Evidence of immense landslides that have occurred on the various islands is presented. Known historical landslide-generated tsunamis in Hawaii are described. Geological evidence of large prehistorical tsunamis generated by landslides are described from the literature. The research using a modeling approach to recreate the generation of tsunamis from mega slides in Hawaii is presented, and compared with the historical evidence.

I. Landslide Generating Tsunamis

Subaerial and submarine landslide-generated tsunamis constitute a class of tsunamis which, although they have caused at least 58,000 fatalities in the last four hundred years, are inadequately studied and generally fall outside current ...mitigation systems. (7-187) In this paper we examine a subset of this class of tsunamis, those generated by landslides in Hawaii.

Tsunamis are most often generated by an impulsive vertical displacement of the water column. Our knowledge of tsunami generation is incomplete. **Studies of tsunami data suggest that the size of a tsunami is directly related to the size and shape of the disrupted area under water, the rate of displacement, the amount of displacement and the depth of the water in the area of generation.** (6-2) In general, a landslide generates a tsunami when the volume of solid material enters the water and bulges up at the toe of the slide displacing the water in an upward direction above the toe of the slide. As a general rule historic landslide-generated tsunamis, while they can be locally devastating, lack the energy to travel large distances. However, the volume of material involved in these slides is relatively small and the amount of ocean displacement is correspondingly small. (7-191)

The basic cause of landslide tsunamis is the failure of over-steepened deposits or slopes above or below the water surface. Once unstable conditions exist the failure can be triggered by any of several agents such as earthquakes, volcanic activity, rain (which increases the mass and reduces the friction), and continued deposition or progressive failure from creep. Once the slide material has been released, the resulting wave depends on the kinetic energy in the slide, the volume and geometry of the affected body of water, and other factors such as the depth of water in the slide area. When subaerial landslides impact a body of water, both a surge or splash and a tsunami are generated. The surge is not part of the tsunami as defined here since its velocity is kinetically-generated rather than gravitational in nature. Its velocity does not depend on the depth of the body of water. However, the displacement of the water does create a true tsunami in addition to the splash. (7-188)

For example, on July 10, 1958, a M_s magnitude 7.9 earthquake set in motion a 30 million m^3 slide that was released from 200-1000 m above Gilbert Inlet, Lituya Bay, southern Alaska, and sped down slopes of about 40° on the east side of the inlet. The impact of the slide on the water sent a surge (splash) across the inlet to the opposite point of land, clearing the forest to a height of 524 m. The resulting tsunami was 30 to 50 meters high near the middle of Lituya Bay. (7-189) The tsunami overtopped Cenotaph Island and La Chausse Spit at the mouth of the bay clearing trees as it passed over. The wave collapsed when it reached the open Pacific. It was barely recorded in Hilo, Hawaii, with a peak-to-trough height of 0.1 m (6-101).

Collapses of volcanic edifices have also generated documented tsunamis. In fact, of eleven volcanic events that generated large tsunamis, eight of these were connected with some type of major deformation of the volcano itself. (9-4) In 1792, a 535 million m^3 portion of Unzen Volcano, Japan, collapsed. The collapsed area was located some 4 km from the vents which had been active a month or two earlier. The "cold" collapse and resulting landslide were probably caused by an earthquake "swarm" that acompanied the withdrawal of magma from the magma chamber within the volcano. The landslide-generated waves reached a height of about 10 m and caused devastation for a distance of 77 km along the Shimabara peninsula on north Kyushu Island. Fifteen thousand people were killed or disappeared without a trace, and 6,200 houses were destroyed. (7-190)

An explosion on October 6, 1883, of the summit of the St. Augustine volcano in Alaska generated a debris avalanche which, in turn produced a tsunami wave of 7.6 to 9.1 m. It reached English Bay (85 km to the east) about 25 minutes later and nearly destroyed the community. (7-190)

II. Documented Landslide-related Tsunami Events in Hawaii

There have been a number of tsunami events in Hawaii in historical times that have landslides as their generating mechanism. On October 2, 1919, an eruption of Mauna Loa produced a stream of lava

which reached the sea near Alika, creating a delta. The submarine extension of the flow became unstable in the marine environment and collapsed beneath the sea surface, creating a 4.3 m wave which caused minor damage and swept several people out to sea. They were later rescued. (7-190)

Subsidence and perhaps an offshore landslide played a part in a tsunami that occurred on the Island of Hawaii on April 2, 1868. Subsidence on the entire southeastern shore of the island was accompanied by an earthquake. This earthquake was apparently related to the incremental movement of a giant slump (14-259) The tsunami associated with the event rose to a height of 20 m and deposited rubbish and timber inland a distance of 0.4 km. This tsunami resulted in 47 deaths in Hawaii. The waves were measured on the west coast of the United States about five hours later but were only about 10 cm in height (San Diego). (3-102)

More than one hundred years later on November 29, 1975, a sudden movement of the seafloor off the southeast coast of Hawaii accompanied a M_s 7.2 magnitude earthquake. Coincident with the earthquake, a 60 km length of Kilauea's south shoreline subsided more than a meter. The wave height in this area was 7.6 m and may have been augmented by the subsidence. Of 32 campers in this area, 19 were injured and 2 were killed. (3-107) Like the 1868 event, the 1975 event may have been related to movement on a slump that was deeply rooted in the volcanic edifice and may have extended back to the volcanic rift zone reaching a thickness of 10 km. A 60 km length of Kilauea's south coast subsided 3.5 m and moved seaward 8 m. The material involved in these slumps may have abruptly surged forward resulting in the earthquakes and the tsunamis. (12-127)

III. Prehistorical Landslides on Volcanic Islands

Recent sonar imagery reveals that this type of movement of large portions of the volcanic edifices has occurred not once but repeatedly in Hawaii. About 70 major landslides over 20 km in length were detected by *Gloria* sidescan sonar studies done in the 1980s. Some of these slides attain lengths of almost 250 km along the seafloor of the Hawaiian Deep, and volumes exceed 5,000 km³. They are among the largest slides on the planet. (13-46). All are traceable back to the steep slopes of the volcanoes from which they slid. The larger deposits are estimated to have volumes of about 5,000 km³. For a typical volcano, this implies that the equivalent of a block 20 km by 20 km or more in area and the full depth of the edifice has been removed. (2-195)

A. Mechanism of Prehistorical Landslide Formation

How did such large movements of material on the perimeters of the volcanic edifices come about? Each of the volcanoes in the Hawaiian chain were born on the ocean floor. As the magma reached the opening in the neck of the volcano, it was spewed out on the floor of the ocean. This quick-cooling of the magma resulted in the formation of crumbly pillow lava. This process continued until the volcano reached the surface of the sea. Then the extruded lava formed a hard, heavy cap over a build-up of thousands of meters of crumbly, steam-shattered, volcanic debris that was erupted beneath the surface of the sea. As the volcano grew it also spread out and sank in response to the pull of gravity. The lava continued to build the volcano adding weight to the top. When the pressure of the weight of material on top exceeded the strength of the crumbly material below, a portion of the edifice failed. Renewed volcanic activity may result when the pressure of the cap over areas of volcanic activity is relieved. One failure model argues that the pressure of magma in dikes pushes the edifice outward, causing the oversteepening of the volcano's slopes that in turn results in slumping and landsliding. Another model suggests that the height of the volcano is the fundamental variable in determining the sliding potential. An increase in height produces a similar increase in the steepness of the slope and in the weight of material resting on the volcano's crumbly interior. (2-195, 196) The largest landslides apparently occur late in the period of active shield growth when the volcanoes are close to their maximum size, but are still active with growth and with seismic activity. (12-125)

Volcanoes, particularly those with steep slopes and those that have bases below sea level, are likely to have internal features that reflect numerous surfaces of slip and large regions of internal instability. Molten rock and fractures also produce areas of weakness. A volcano contains many natural break points upon which several types of landslides or debris flows can occur.

On a smaller, more localized level, debris avalanches, like those that occurred at the Mount St. Helens eruption may tumble down the submerged flanks of the volcanic islands generating local tsunamis. These medium sized landslides having volumes measuring tens of cubic kilometers are common in shallower water. (12-125) Debris avalanches affect more limited areas on the surface of island flanks than do the giant slumps. These avalanches are longer, thinner, and not as steep. Hummocky terrain containing larger unbroken blocks of the slides is found in the outermost part of the slide area. The distal end often moves up the slope of the Hawaiian Arch for distances as much as tens of kilometers. These debris avalanches resemble the volcanic landslides produced in 1980 at Mount St. Helens, and must have moved rapidly as did the material in the Mount St. Helens avalanche. (12-131) This type of rapid movement of material into and beneath the surface of the sea would undoubtedly have produced a tsunami.

Rapidly moving avalanches that move blocks up to 10 km in size for distances of up to ten meters would produce major disturbances in the water column which could generate giant tsunamis (13-46). Some slides have been known to plunge into the sea with enough momentum to spread material more than 166.7 km across the ocean floor (4-33,34) or even down into the Hawaiian Trough and up the flank of the Hawaiian Arch.

On a much larger (and also more infrequent) scale a third or more of an entire island can sink (and has) beneath the waves in a single slide. Such island blocks may reach 20-30 km in dimension and two to three km in thickness. (1- 287) This greater threat is posed by the vertical movement of large segments of the volcano itself near its base that can generate earthquakes far more powerful than those "volcanic" earthquakes that accompany movement of the magma within the edifices. In cases where a large section of the underwater portion of the volcano is displaced, the potential for the generation of very large tsunami-like waves that may pose a serious threat to coastal areas far from the islands themselves. (2-196) . The largest of these landslides take place when a volcano grows to maximum size. They occur with inter-event times of around 300,000 or 400,000 years. (4-33,34)

B. Specific examples of Prehistorical Large Landslides
1. In Hawaii
a. Big Island
'Alika Slide This, most recent of the huge Hawaiian slides, probably slipped off the west flank of Mauna Loa Volcano 105,000 years ago. The huge cliff to the north in Pu'uhonua O Honaunau National Historical Park is probably the scarp of this enormous landslide. The landslide may have generated the giant tsunami that scrubbed the soil off the island of Kaho'olaw to the height of 242 meters and washed blocks of coral even higher up the side of the island of Lana'i. (4-105)

The Ninole Hills may be eroded remnants of an older version of Mauna Loa that collapsed thousands of years ago. A giant landslide may have torn away the southern flanks of these hills. (4-99)

Big slices of Kilauea's south flank are slumping into the ocean along a series of faults. Some of the scarps are as much as a 300 meters high. Occasional swarms of earthquakes confirm the continuing collapse. Submarine surveys show the area measures 83 km long and 67 km wide. (4-53)

b. Lana'i
Clark Slide. A landslide may have completely removed the former summit of Lana'i, and the present island appears to be the northeastern flank of a once much larger volcano. Sonar maps of the ocean floor reveal a large rock mass stretching nearly 116.7 km from the southwest coast of Lana'i spreading into two huge lobes where it enters the Hawaiian Deep. This great distance suggests that the material must have been moving very fast. (4-176) A steep face of a 136.4 meter-high bench along the eastern edge of Palawai Basin is thought to be one of the

headwall scarps of the Clark Slide. If so, a big piece of the western side of Lana'i also dropped as much as 41 meters, but not into the ocean. (4-177)

c. Moloka'i

Wailau Slide. As volcanic activity came to an end, the northern half of the caldera on East Moloka'i disappeared into the ocean in the Wailau Slide. That the slide was moving rapidly is evidenced by the fact that it scattered fragments nearly 166.7 km north across the Hawaiian Deep, in a strip 41.7 km wide. (4-192, 193) The scar it left behind is the towering sea cliff along the island's north shore, the highest and quite possibly the most spectacular shoreline cliff in the world (Kalauupapa Overlook). It rises almost vertically 1,121 meters out of the sea. Islets and sea stacks along the base show that waves have eroded the cliff at least a short distance inland. Large stream valleys have cut across the cliff face to a depth of nearly 1,818 meters below present day sea level. They were eroded when the island stood much higher, and became submerged as it sank. Obviously, the great cliff was then 1,818 meters higher, too. Adding the distance the scarp extends above sea level (1,121 m) to the depth of the stream valley would put the height of the great landslide scarp at over 2,727 meters! The Wailau Slide is the third largest slide identified in Hawaiian waters, after the North Kaua'i and Nu'uanu slides. According to James Moore (U.S. Geological Survey) the volume of the slide corresponds to the amount of lava the Hawaiian hot spot would erupt in 10,000 years at its current rate. (4-192)

d. O'ahu

Ka'ena Slide. The north flank of Wai'anae on the leeward coast of Oahu was also unstable. The Ka'ena Slide moved nearly 116.7 km across the deep ocean floor and formed an underwater escarpment parallel to the North Shore between Ka'ena Point and Waialua. The distance traveled by this slide indicated that it must have been traveling extremely fast. This slide may have been a catastrophic event, the kind that generates enormous tsunamis. (4-210)

Nu'uanu Slide. The unsupported eastern flank of Ko'olau Volcano sloped steeply into the deep ocean. This steep eastern flank on Ko'olau must have swelled as magma rose into the volcano, then deflated as it erupted. Those movements may have helped destabilize the eastern flank enough to cause the Nu'uanu Slide, one of the largest known slides on Earth. It amputated a large area of eastern O'ahu and sped across the sea floor, laying down a bed of rubble 3.3 m wide and extending for 200 km and up the slope of the Hawaiian Arch. A single block in this slide debris is 30 km long and 1.7 km wide. The size of the fragments and the distance that they traveled indicate great momentum and speed—both conditions needed for tsunami generation. (4-212)

e. Kaua'i

Sonar seems to show large pieces that broke off the eastern part of the island and slid into the ocean. One mass moved north, the other south. Debris from them swept up the slope of the Hawaiian Arch, as far as 100 km from Kaua'i. Rapid movement appears to offer the best explanation for the sonar features. (4-255, 256)

f. Ni'ihau

Ni'ihau was once a much larger island, as is evidenced by the towering cliff on the eastern flank of the Island. The cliff is the headwall of a slide that detached a large section of the island and dumped it into the ocean hundreds of thousands of years ago. Only a small remnant of the original western flank remains above sea level. (4-285)

2. On other Marine Volcanic Islands

Hawaii is not the only place where such giant earth movements may have taken place. Multi-beam bathymetric maps reveal evidence of numerous large scale landslides on the Emperor and Michelson

Ridges, on the Map Makers and Marcus-Wake sea mounts. Re-examination of *Gloria* images has shown the presence of landslides on the submarine slopes of the Canary Islands and Tristan de Chuna. The Marquesas volcanoes also appear to have undergone major collapses. These landslides have occurred on the flanks of oceanic volcanoes regardless of island size, geologic age, and climate. (12-141)

C. Modeling of Prehistorical Landslides in Hawaii

Caution must be exercised, however, in concluding that these huge landslides will, when they occur, generate very large tsunamis. Using modeling techniques Jones and Mader found that "for the assumed landslide model to obtain the necessary run-up, a volume of 1,600 km^3 greater than twice the likely volume of the Alika 2 debris avalanche is required." (5-46) LeBlond and Jones further conclude that an error is introduced when calculations of the size of tsunami waves generated assume that the landsliding mass behaved like a rigid body. (8-25)

IV. Giant Slide Generated Tsunamis

A. In Hawaii

Is there evidence that such giant tsunamis or waves have been generated by landslides in Hawaii? In 1984, Moore and Moore identified tsunami-like deposits almost 400 m above sea level on the Hawaiian island of Lana'i. The Hulope Gravel is a deposit of boulders, coral fragments, and calcareous beach rock slabs. Near the top of the deposit are sand and shell fragments. Remains of this deposit can be found at 375 m on the Island of Lanai. (11-1312) The Hulope Gravel consists of three beds each two to four meters thick which may have been laid down by successive waves. (10-101)

### B. In Areas Remote to Hawaii

Young and Bryant proposed that erosive features found along the sea shore of southeastern Australia, 7,000 km away were produced by the same giant wave that deposited the Hulope Gravel. (15-199) They state: "Sand barriers along the coast of southern New South Wales, dating from the last interglacial period, have been almost completely destroyed, most probably by a catastrophic tsunami. Evidence for catastrophic wave erosion can also be traced to heights of at least 15 m above present sea level on coastal abrasion ramps. These erosional features lie above the range of effective erosion by contemporary storm waves and cannot be attributed to [fluctuations in sea level.] Chronological evidence for the timing of the destruction of the last interglacial barriers suggests that tsunamis generated by the submarine slide off Lanai in the Hawaiian Islands 105 ka traveled across the Pacific and eroded this coast." (15-199)

V. Potential for Slides of the Future to Generate large Tsunamis

The volume of the slide into Lituya Bay that generated a 50 m tsunami locally was 30 million m^3 while the slides off the shores of Hawaii are up to (125 billion m^3) 5,000 km^3 in size. The size of the debris avalanches (landslides) that have occurred in Hawaii are one hundred thousand times the volume that occurred in this slide. The slide at Unzen Volcano that generated a tsunami that, in turn, killed 15,000 people at Shimabara, Japan, is dwarfed by these volcanic slides and slumps. (535 million m^3 as opposed to [125 billion m3] 5,000 km^3) It is true that the slide into Lituya Bay hardly generated a ripple outside that bay, but what if the slide had been a [a thousand] hundred thousand times bigger? And what if it had occurred in the open ocean instead of an enclosed bay? It is difficult to believe that coastal areas on the perimeter of the ocean basin would not have been effected. The speed with which the ocean floor is changed is also certainly an important factor in tsunami generation. Many of these slides appear to have traveled at great speeds. Obviously these events are very rare. However, when one takes into consideration the number of volcanic islands in the oceans of Earth and the massive potential size of the slides, the tsunami threat becomes one that cannot be ignored. Clearly one must exercise caution when concluding that huge tsunamis have been generated in Hawaii by landslides and slumps. However, taking into consideration the historical evidence alone certainly brings one to the conclusion that such tsunamis would, at least, be locally devastating. Recall that the work of Young and Bryant suggests that they have found evidence on the southeastern coast of Australia that giant waves generated in the Hawaiian Islands may have traveled to shores more than 7,000 km away.

References

1. Borgia, A. & B. Treves, 1992. Volcanic plates overriding the ocean crust; structure and dynamics of Hawaiian volcanoes, *Ophiolites and their Modern Oceanic Analogues, Geological Society Special Publication, No. 60,* The Geological Society, London, 60:277-299.

2. Delaney, Paul T., May 1992. You can pile it only so high, *Nature,* Vol. 357:194,195.

3. Dudley, Walter C. and Min Lee, 1988. *Tsunami!,* University of Hawaii Press, Honolulu, Hawaii,.

4. Hazlett, Richard W. and Donald W. Hyndman, 1996. *Roadside Geology of Hawaii,* Mountain Press Publishing Company, Missoula, Montana.

5. Jones, Anthony T. and Charles L. Mader, 1995. Modeling of tsunami propagation directed at wave erosion on southeastern Australia coast 105,000 years ago, *Science of Tsunami Hazards,* The Tsunami Society, 13:45-53.

6. Lander, James F. and Patricia A. Lockridge, August 1989. *United States Tsunamis (Including United States Possessions), 1690-1988,* National Geophysical Data Center.

7. Lander, James F., Patricia A. Lockridge, and Herbert Meyers, 1988. Subaerial and Submarine Landslide Generated Tsunamis, *Panel of Wind and Seismic Effects, US-Japan,* U.S. Department of Commerce, National Bureau of Standards NGISR- 88-37703, Gaithersburg, MD, p. 187-199.

8. LeBlond, Paul H. and Anthony T. Jones, 1995. Underwater landslides ineffective at tsunami generation. *Science of Tsunami Hazards,* The Tsunami Society 13:25-26.

9. Lockridge, Patricia A., Non-Seismic Phenomena in the Generation and Augmentation of Tsunamis, Unpublished Manuscript.

10. Moore, George W. and James G. Moore, 1988. Large-scale bedforms in boulder gravel produced by giant waves in Hawaii.. *Geological Society of America, Special Paper* 229:101-110.

11. Moore, James G., and George W. Moore, 1984. Deposit from a Giant Wave on the Island of Lanai, Hawaii, *Science,* 226:1312-1315.

12. Moore, James G., William R. Normark, and Robin T. Holcomb, 1994. Giant Hawaiian Landslides, *Annual Review of Earth and Planetary Science,* 22:119-144.

13. Moore, James G., William R. Normark, and Robin T. Holcomb, April 1994. Giant Hawaiian Underwater Landslides, *Science,* 264:46,47.

14. Moore, J.G. and R. K. Mark, 1992. Morphology of the Island of Hawaii, *GSA Today,* 2:257-59.

15. Young, R.W. and E.A. Bryant, March, 1992. Catastrophic wave erosion on the southeastern coast of Australia: Impact of the Lanai tsunamis ca. 105 ka? *Geology,* 20:199-202.
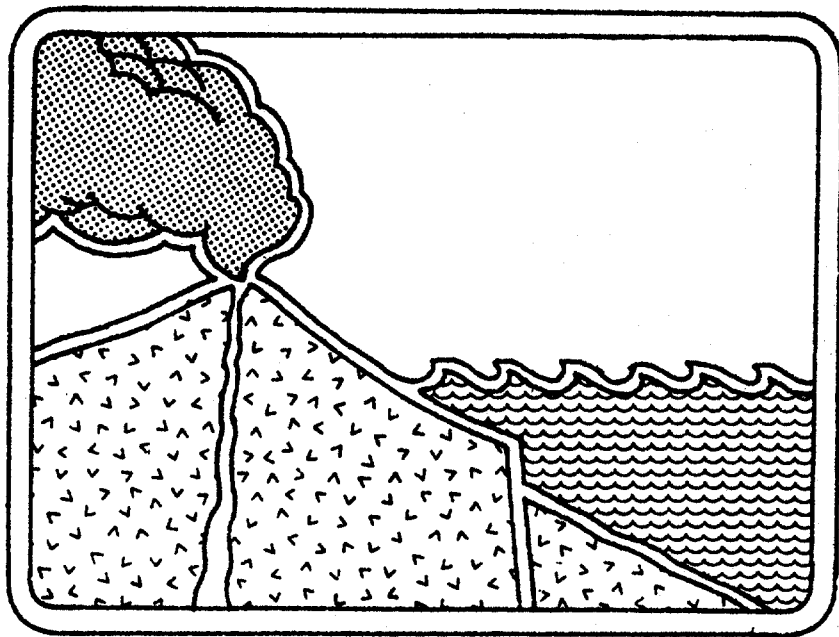
THE NEW TSUNAMI WARNING SYSTEM OF
THE JAPAN METEROLOGICAL AGENCY

Hidee Tatehata

Earthquake and Tsunami Observation Division

Seismological and Volcanological Department

Japan Meterological Agency

1-3-4 Ote-machi, Chiyoda-ku, Tokyo 100 Japan

ABSTRACT

Since 1941, the Japan Meterological Agency (JMA) has conducted tsunami forcasting for our country, which frequently has suffered considerable losses from tsunamis. However, huge tsunamis still cause damage and kill many people; for example, the Japan Sea Earthquake Tsunami (May 26, 1983, M=7.7) and the Hokkaido Nanseioki Tsunami (July 12, 1993, M=7.8). These experiences caused the development of more prompt and accurate tsunami forecasting for the purpose of survival, as in Darwin's Theory of Evolution. The new system has the following three sections:

- New seismograph network and P-wave magnitude determination.
- Rapid interpolation numerical tsunami model.
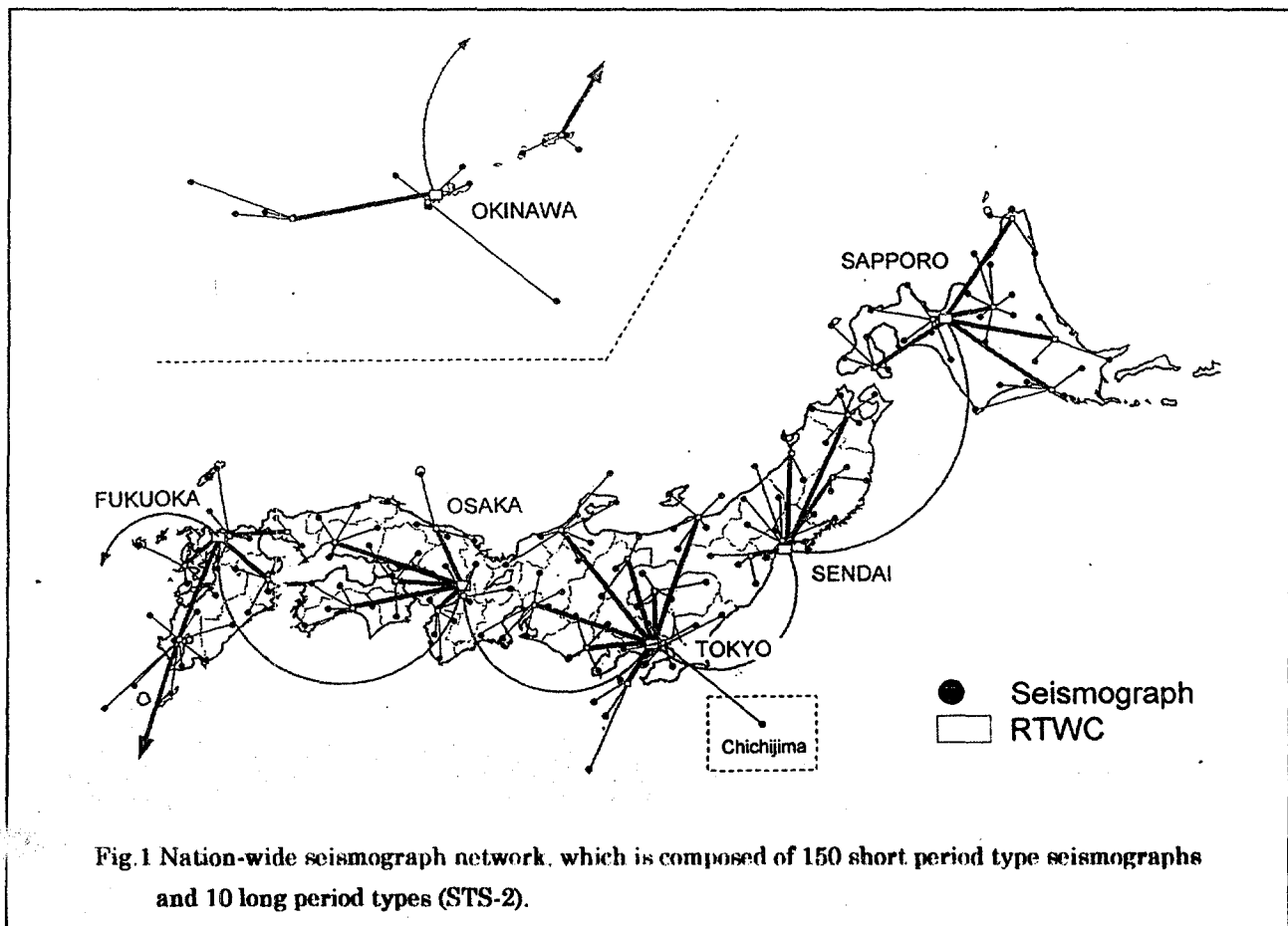- Satellite based system for dissemination of information.

The establishment of the new seismograph network and the satellite-based dissemination system were completed in 1994. The fast numerical tsunami model is scheduled to be completed within a few years. In this paper, the new system and procedures are described, especially the fast numerical tsunami model in detail, because it should be the first real-time application of a numerical tsunami forcast in the world. Recently, the fast calculation and accuracy of tsunami forcast by this numerical model has been confirmed through the analysis of historical tsunami records.

1 Introduction

In the case of Hokkaido-Nansei-Oki-Earthquake (July, 12,1993, M=7.8), the Okushiri island was severely attacked by the huge tsunami waves with 230 dead or missed persons, within about three minutes after the occurrence of the earthquake. Unfortunately, due to the limitation of the ability of the existing system, the issuance of tsunami warnings was impossible. The project to establish new system and procedures for the more quick issuance of warnings aiming at the dissemination within 3 minutes after the occurrence of the big earthquake has been conducted since April 1994 by the Japan Meteorological Agency (JMA). This system and procedure have been completed in 1995. And at the final stage of the project, the numerical tsunami model will be added and operated.

2 New Seismograph Network and P-wave Magnitude

For the purpose of shortening the time to locate an earthquake and to estimate its magnitude, the JMA has deployed the seismological network composed of 150 high sensitivity seismographs and 20 STS-2 models throughout Japan in March 1994 (Fig.1). The system for tsunami forecast continuously receives real-time seismic data at stations, and automatically determines the magnitude and the location of an earthquake using arrival time and waveforms of P-waves respectively.

Fig.1 Nation-wide seismograph network, which is composed of 150 short period type seismographs and 10 long period types (STS-2).

P-wave magnitude

According to the elastic wave theory, far field source-time function is expressed as convolution of the dislocation velocity and rupture velocity. Seismic moment corresponds to the area of the far field source-time function. The far field P-wave displacement is given as follows;

$$u = \frac{Rp}{4 \pi \rho V^3 r} \; g(\Delta)s(t)^*Q(t)^*I(t)$$

where ρ is density, V is P-wave velocity, r is distance between source and seismometer, Δ is angular distance, $g(\Delta)$ is geometrical spreading factor, $s(t)$ is source time function, $Q(t)$ is attenuation factor and $I(t)$ is instrument response of seismometer respectively.

In case of a large earthquake of which magnitude is greater than 7, the order of duration time is 10^1 seconds. A broad band seismograph has flat response for a period longer than 10 sec, and the area of the far-field wave(S) is proportional to the seismic moment(Mo) as shown below;

$$\log(Mo)=k \cdot \log(S) \qquad (\text{I})$$

where k is constant value.

Kanamori(1983) defined moment magnitude (Mw) as follows;

$$\log(Mo)=1.5 \cdot Mw+16.1. \qquad (\text{II})$$

By the combing the equations I, II and assuming P-wave magnitude(Mp) equal to Mw, following equation is derived;

$$Mp=a \cdot \log(S)+b \cdot \log(\Delta)+c. \qquad (\text{III})$$

In addition, there is a proportional relationship between S and the maximum amplitude(A) of P-wave displacement data. Although the radiation pattern and path effects ought not to be ignored for the determination of magnitude, these factors can be neglected for the practical use.
Therefore, the JMA decided the following equation(a,b,c), instead of equation(III),

$$Mp = a \cdot \log(A)+b \cdot \log(\Delta)+c.$$

And the coefficients (a,b,c) were determined to minimize

$$| M_{jma}-(a \cdot \log(A)+b \cdot \log(\Delta)+c) | .$$

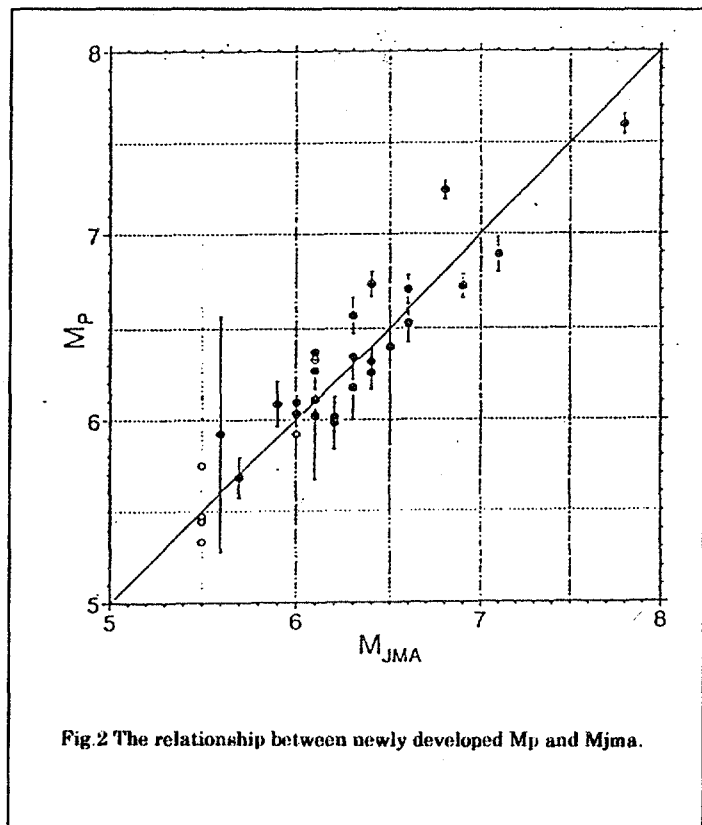Fig.2 The relationship between newly developed Mp and Mjma.

Fig.2 shows the relationship M_{jma} and Mp.

Open and closed circles denote Mp determined with only one station and multi stations respectively. Error bar of one sigma is also shown. Overall these two magnitudes fit quite well.

After the establishment of the new seismograph network and the operation of the algorithm for automated determination of Mp, the Hokkaido-Toho-Oki Earthquake occurred on October 4,1994. This event was a good example to examine the abilities of this system. The JMA could issue Tsunami warning in 5 minutes after the occurrence, in spite of this event occurred outside the network; it took several tries to get the final epicenter location.

Its Mp was automatically calculated by using P-waves with 40 sec period, the final Mp obtained to be 8.2. This value is well consistent with M_{jma}(8.1) and with Mw(8.3) determined by Harvard University Group. It can be concluded that the adoption of Mp, the JMA can quickly evaluate whether a tsunami may be generated by the earthquake.

3 Rapid Numerical Tsunami Model

The JMA is developing the new tsunami forecast methods using the database for the various kinds of results calculated by the new numerical tsunami model. With these accurate tsunami forecast procedures, the dissemination of accurate height and arrival time of tsunami in the respective areas are planned for all Japanese prefectures. In order to take refuge from tsunami, this information will be very important for the people affected by tsunami disasters. However, it needs a high-speed processing numerical model to issue a tsunami warning prior to arrival time of the tsunami. The abilities required are as follows:

Elapse Time : Within 1 second after the determination of the hypocenter and magnitude,

Forecast Range : In 2000km compass from the tsunami source

Region size : About 100~200km. (approximately equivalent to the size of each prefectures in Japan).

3-1 Methods.

The JMA installed a computation system for tsunami forecast in 1981, but the system has been equipped with neither a high-speed computer nor a numerical tsunami model. So, the JMA originated a unique numerical tsunami model based on basic mathematics.

There is a general approximation formula about a nonlinear function as follows:

$$f(x) \fallingdotseq f(x_0) \times (1-k) + f(x_1) \times k,$$

where x is in the range [x0 , x1] and is divided the x0 and x1 with a ratio of k:(1-k), respectively. This formula means that the approximate values of f(x) can be quickly obtained by using f(x0) and f(x1), instead of calculating f(x). This formula is a first-degree linear approximation formula. This meaning can be expressed as follows: If there are two results of the tsunami computation for two earthquakes of same magnitude but different hypocenters (x0, x1), and the

distance is close to make this approximation formula applicable, then the wave heights can be represented as f(x0) and f(x1). When another tsunami occurs at the hypocenter (x) where divided with k:(1-k), tsunami height f(x) will be estimated easily with this approximation formula. It is easy to expand this approximation theory into the X-Y coordinates as is clear from the Fig.3. In the same way, the wave heights or tsunami arrival times of any tsunamis generated in the four hypocenters can be estimated with the next approximation formula:

$$f(x,y)=(1-l)\{(1-k)f(x_0,y_0)+k\ f(x_1,y_0)\}+l\{(1-k)$$
$$f(x_0,y_1)+k\ f(x_1,y_1)\}.$$

As an expansion of this theory, the approximation formula does not include only any hypocenters but also magnitude, fault depth and etc. But it is needless to say that a great number of the tsunami simulations are required to make precise forecast for all of the earthquakes and generated tsunamis around Japan like as shown in schematic Fig.4. A white circle denotes a hypocenter for the tsunami simulation.

Specifically, many tsunami simulation output files are fulfilled as in Fig.5. A white circle means a data file related to the tsunami heights for the entire coast in Japan.
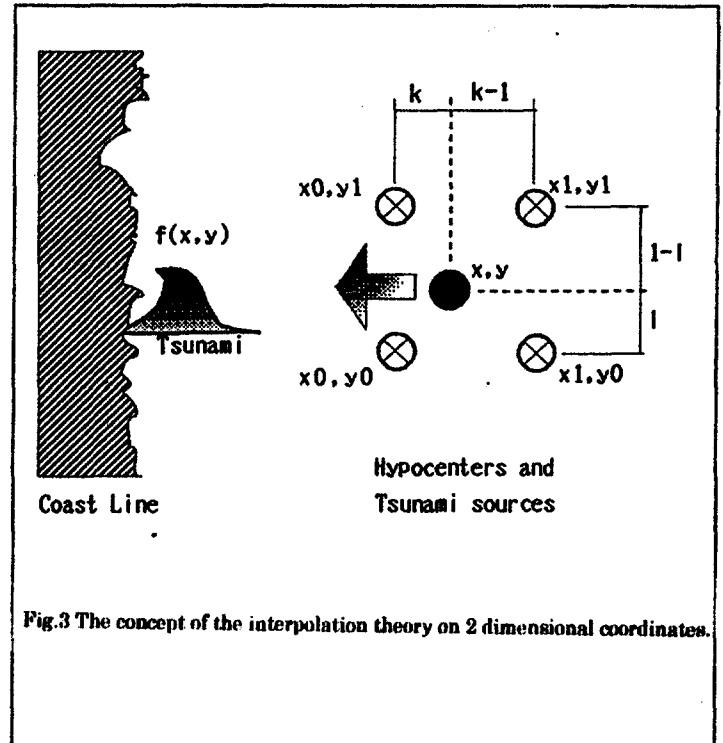
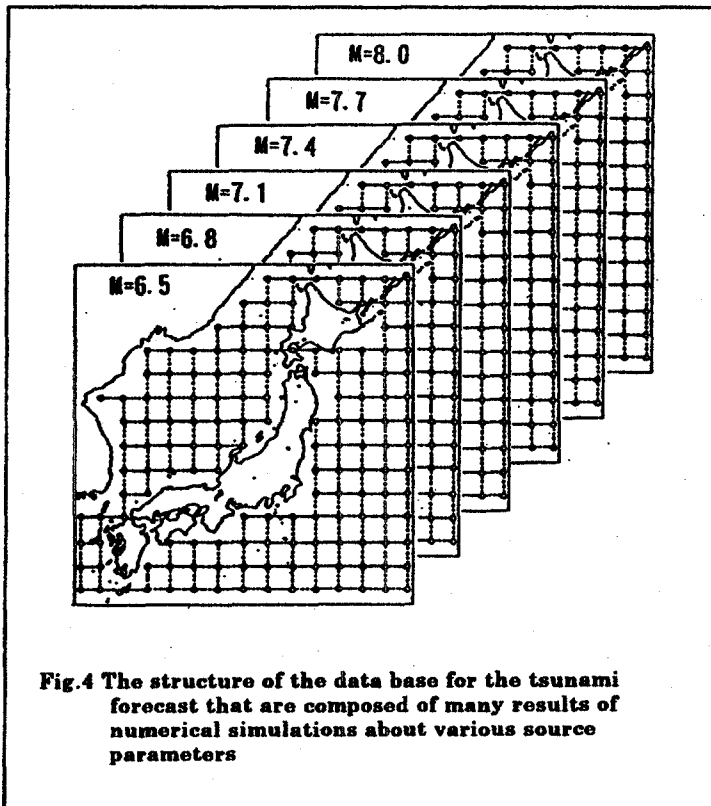Fig.3 The concept of the interpolation theory on 2 dimensional coordinates.

Fig.4 The structure of the data base for the tsunami forecast that are composed of many results of numerical simulations about various source parameters

Hx= [(1- l){(1- k)h000+ kh100}+ l{(1- k)h010+ kh110}] $^{1-m}$
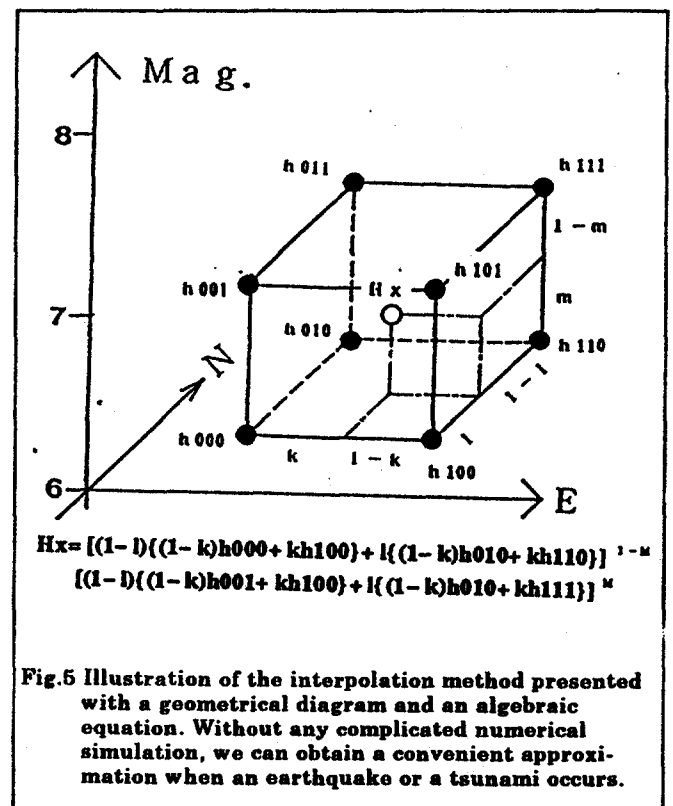[(1- l){(1- k)h001+ kh100}+ l{(1- k)h010+ kh111}] ^{m}

Fig.5 Illustration of the interpolation method presented with a geometrical diagram and an algebraic equation. Without any complicated numerical simulation, we can obtain a convenient approximation when an earthquake or a tsunami occurs.

When an earthquake large enough to generate a tsunami occurs, the tsunami forecast system searches the eight data files which have results of numerical simulations for the earthquakes at closest hypocenter and having similar magnitude. Then, by use of linear approximation/interpolation among them as shown in Fig.5, the system determines the tsunami estimation. But, the estimation of displacement of seabed or tsunami heights needs consideration epicenter's depth. Therefore, Fig.4 has to be expressed in four-dimensional coordinates. For the practical operations, the system uses 16 data files. However, the accumulation of these data files containing about 100,000 numerical simulations takes very long CPU time. To construct the data files for all events near Japan, the JMA decided to use the super-computer HITAC-S810-20K which has 630 MFLOPS power and has been mainly used for numerical weather forecasting projects. The JMA can now perform these many simulations automatically.

The second problem is on the fault parameters. It is because that the calculation about the dislocation and swelling sea surface needs the fault parameters about the earthquake. Around Japan, however, major earthquakes occur approximately with the fault parallel to the trench axes, as presented in Fig.6.

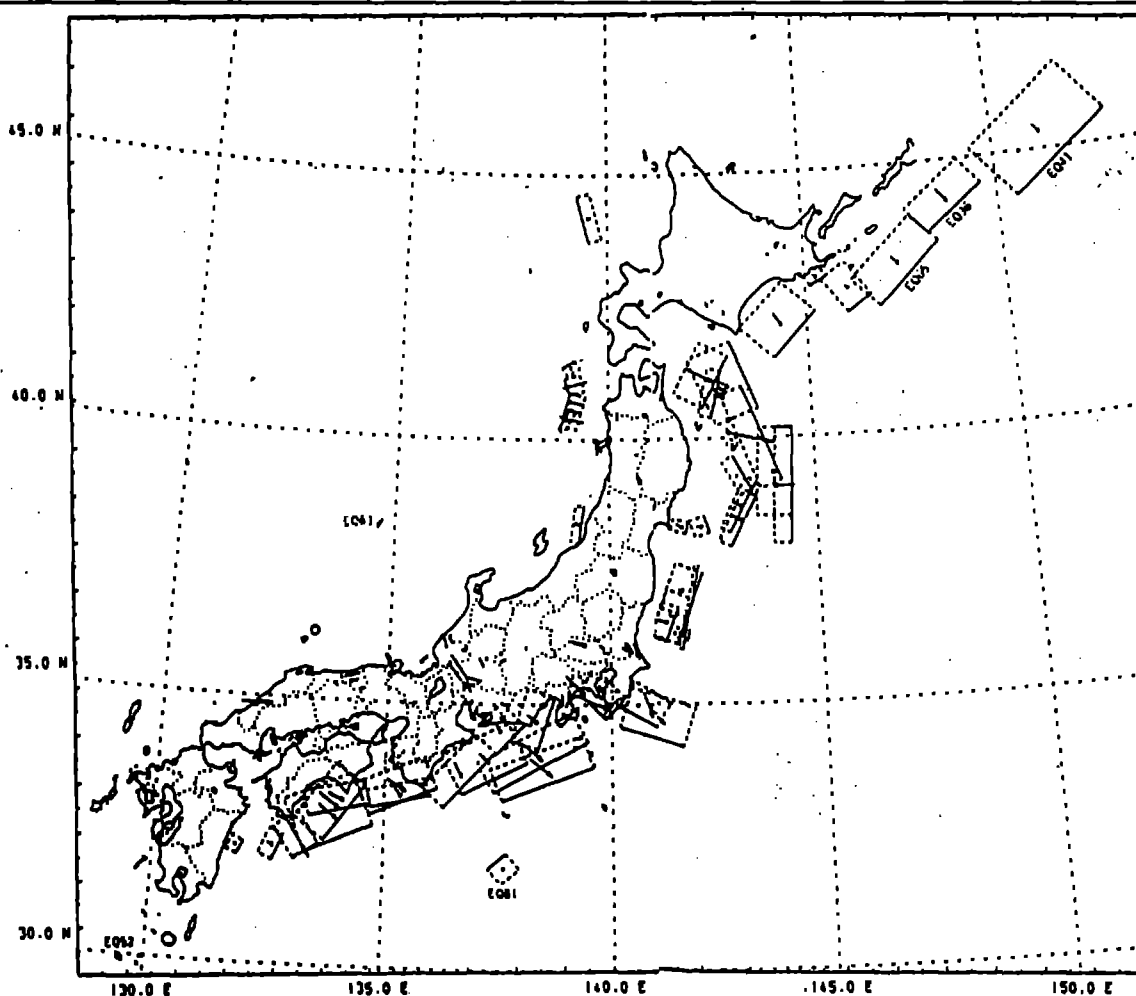In addition, there is the fact that tsunami height is mainly controlled by the quake's magni-

Fig.6 The fault planes around the coast of Japan, which had generated tsunamis in historical ages. The distributions of these fault planes are characterized by a tendency to be parallel width the coast line. It is noticed that many of them are the reverse type faults.

tude. The relationship between the sizes of fault and magnitude is given as follows:

log L(km)=0.5M-1.9,   W≒L/2

log U(cm)=0.5M-1.4

where, L; length of the fault plane, W; width of the fault plane and U; length of the slip vector. For the reliable disaster mitigation/prevention, the computation based on these equations between magnitudes and statistic fault parameters should be accurate.

When all computation has been completed, all of the results obtained are used to construct the database. The structure of this database is similar to that of a crystal. An atom corresponds to one set of computation results. If these atoms are very near, the resulting interpolation among them becomes more accurate. However, the severe problem of this computation is to be expensive. In this computation, the results obtained are the most efficient, when the distance between two hypocenters is nearly equal to the tsunami source area. Therefore, these atoms/sets are spaced every 50km∼100km on the N-E coordinate plane due to the distribution tendency of the faults around Japan(Fig.6).

It is a very remarkable feature that this interpolation algorithm can promptly carry out the analysis of tsunami generation. It is concluded that this numerical tsunami model can provide quickly the tsunami forecast information from the occurrence of large earthquake without the use of a super computer.

3-2 Application to Prior Events

This interpolation numerical model was applied to the tsunami of the 1933 Showa Sanriku earthquake (March, 3,1933, M8.1, 3,064 deaths) as shown in Fig.7. The output of the interpolation numerical model is overlapped with 16 simulations that formed from tsunami's different source (location, Magnitude, fault depth). In order to evaluate the precision of the new model, we used not only this interpolation numerical model, but also ordinary numerical computation. Each result of two computations agreed well with the observation data for the run-up tsunami heights.

The another example is the 1993 Hokkaido-Nansei-oki Earthquake (July 12, 1993 M7.8), and the results are presented in Fig.8. After the occurrence of this tsunami, huge waves very soon attacked the west coast area of Hokkaido, especially at Okushiri Island with over 20 m height waves, and 237 people killed. The observational results and the values computed by the two models are shown in Fig.8 in the same arrangement as those in Fig.7. Fig.8-③ shows that the Interpolation Numerical Model has some tendency to overestimate tsunami height around the source which is close to the coastline. These results can be used for the actual tsunami warning operations to minimize disasters, but it is possible to correct the overestimation by improvement of the database.

These computation tests of the Interpolation Numerical Model are carried out with a personal computer, and computing to obtain output is very fast. Although this computation algorithm requires considerable time to make the database, it was confirmed that this tsunami numerical model, using the data base method, can promptly obtain the tsunami heights expected for tsunami warning or advisory. In case of the 1993 Hokkaido-Nansei-oki earthquake tsunami, the arrival time of tsunami waves was about 3∼5 minutes in Okushiri Island after
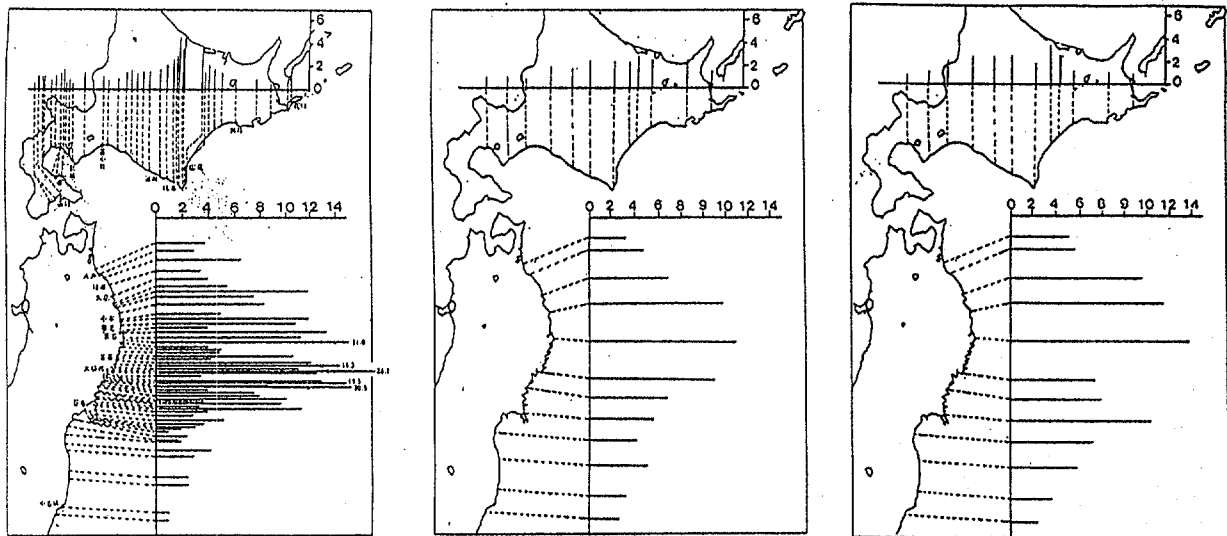
① Observational results   ② Numerical Model output   ③ Interpolation Numerical Model

Fig.7

① Observational results of the tsunami run-up heights by the 1933 Showa-Sanriku-Oki-Earthquake(M=8.1).

② Distribution of the tsunami height obtained by the ordinary numerical model. The fault parameters:
L=180km,W=100km,U=330cm,Slip =-90°,Dip=45° and Normal fault type.
After Kanamori(1971a,1972c)

③ The tsunami heights obtained by Interpolation Numerical Model. Each member of the database is based on the grid points surrounding the hypocenter at distance of 50km. The fault parameter: L=148km,W=74km,U=447cm, Slip=90°,Dip=45° and reverse fault type.
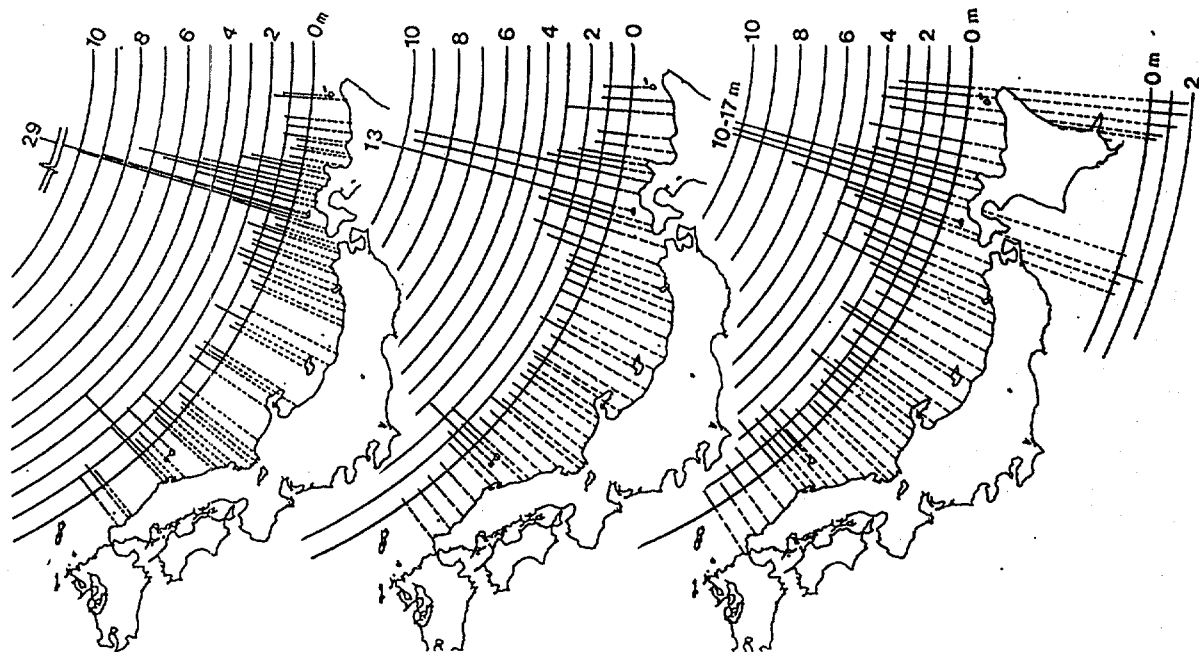
① Observational results   ② Numerical Model output   ③ Interpolation Numerical Model

Fig.8 ① The tsunami run-up heights by the 1993 Hokkaido-Nansei-Oki-Earthquake (M=7.8), based on the JMA's field inspection.

② The tsunami heights computed by the ordinary numerical model. The fault plane parameters by the double fault plane. 1st fault plane L=75km, W=39km, U=300cm, Strike=195°, Slip angle=90° and Dip angle=35°. 2nd fault plane L=75km,W=39km,U=250cm,Strike=165°,Slip angle=165° and Dip angle=35°.
After "The JMA Research Report "(1994)

③ The tsunami heights obtained by the Interpolation Numerical Model. Each member of data base is based on the grid points surrounding the hypocenter at distance on 50km. The faults parameters.L=105km,W=53km,U=316cm,Slip angle=90°,Dip angle=45° and reverse fault type.

occurrence of the quake. Even in such a case, the Interpolation Numerical Model can issue tsunami forecast, and the tsunami warning can be broadcast before the arrival of tsunami waves at the island.

4 Satellite-Based System for Dissemination of Emergency Information

The P-wave magnitude and Interpolation Numerical Model are the new methods to realize the more rapid issuance of tsunami warnings with higher accuracy of the arrival time and wave height. In addition these new methods, it is also important to shorten the transmission time of the tsunami warnings and information from Tsunami Forecasting Centers from the public. The JMA has developed the Satellite-Based Emergency Information Multi-destination Dissemination System and the receiving equipment to be deployed at the prefectural and municipal offices, mass media stations, meteorological observatories/stations, and others as shown in Fig.9. Through this satellite-based transmission system, tsunami warnings and related earthquake information can be directly sent to the receivers immediately after the issuance. The following is the contents of the information contained:

① Tsunami forecast message,

② Seismic intensity,

③ Epicenter and magnitude,

④ Observations of tsunami arrivals and its height,

⑤ Cancel of the tsunami warnings.

This information is broadcast via the Gestational Meteorological Satellite (GMS), and can be
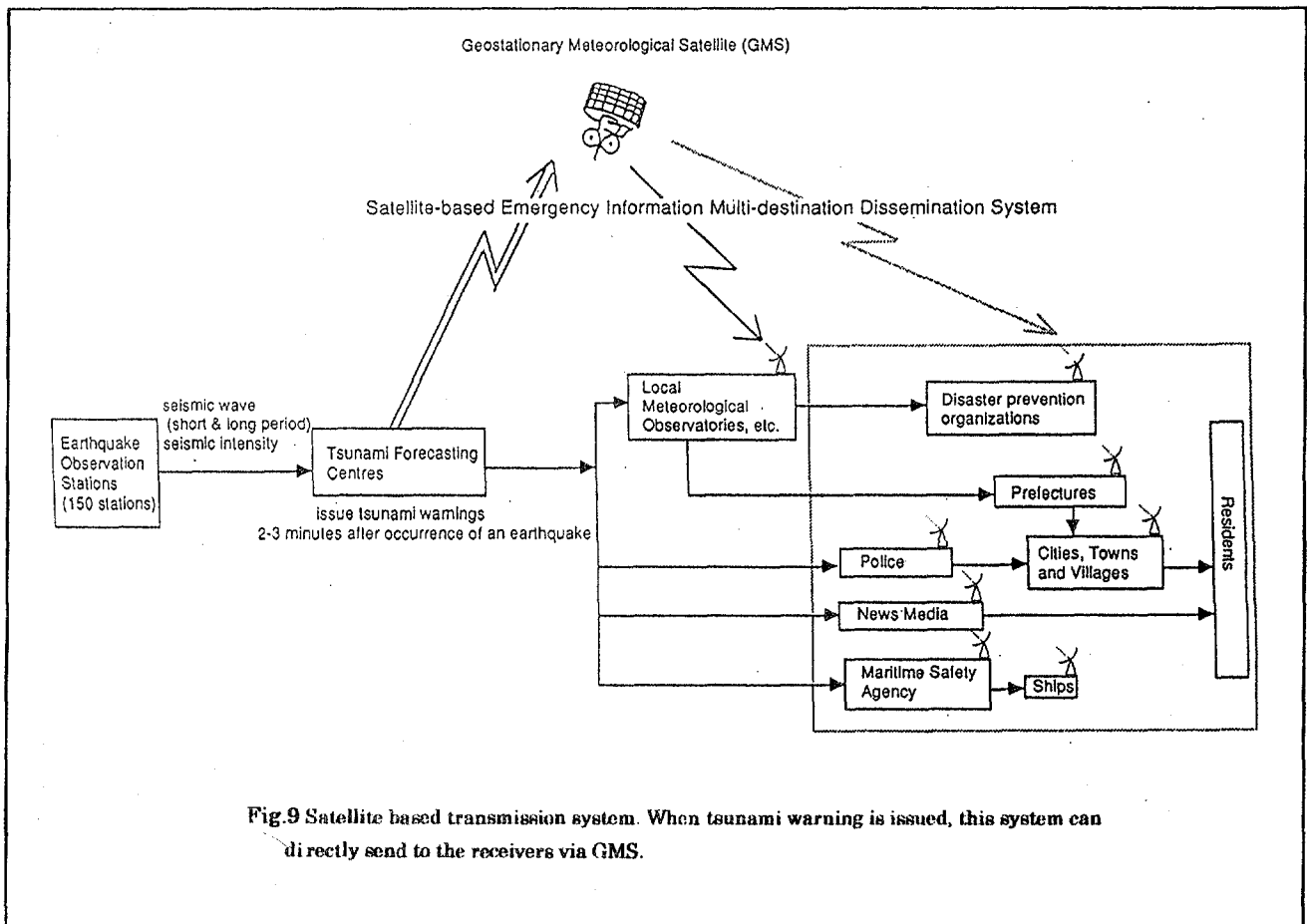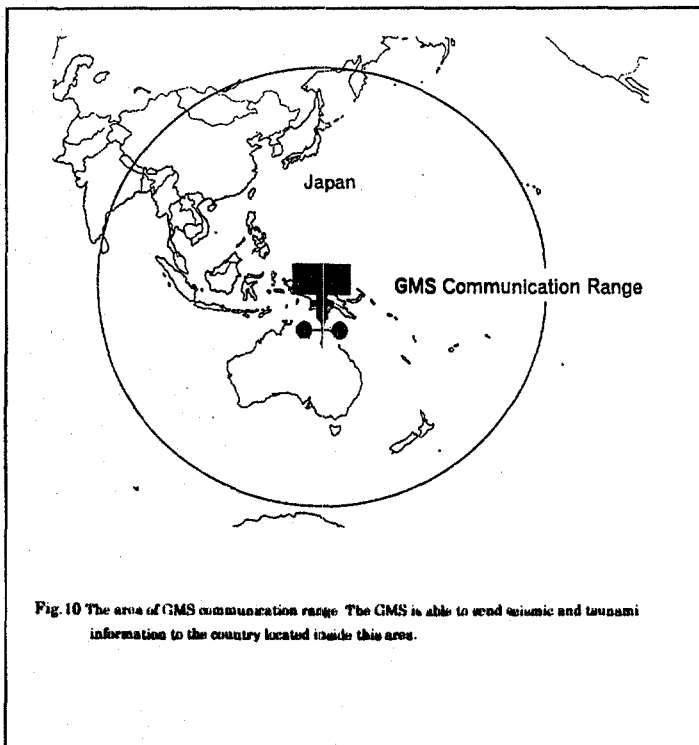

Fig.9 Satellite based transmission system. When tsunami warning is issued, this system can directly send to the receivers via GMS.

received in the area illustrated in Fig.10. The locations in this area may use this information

Fig. 10 The area of GMS communication range. The GMS is able to send seismic and tsunami information to the country located inside this area.
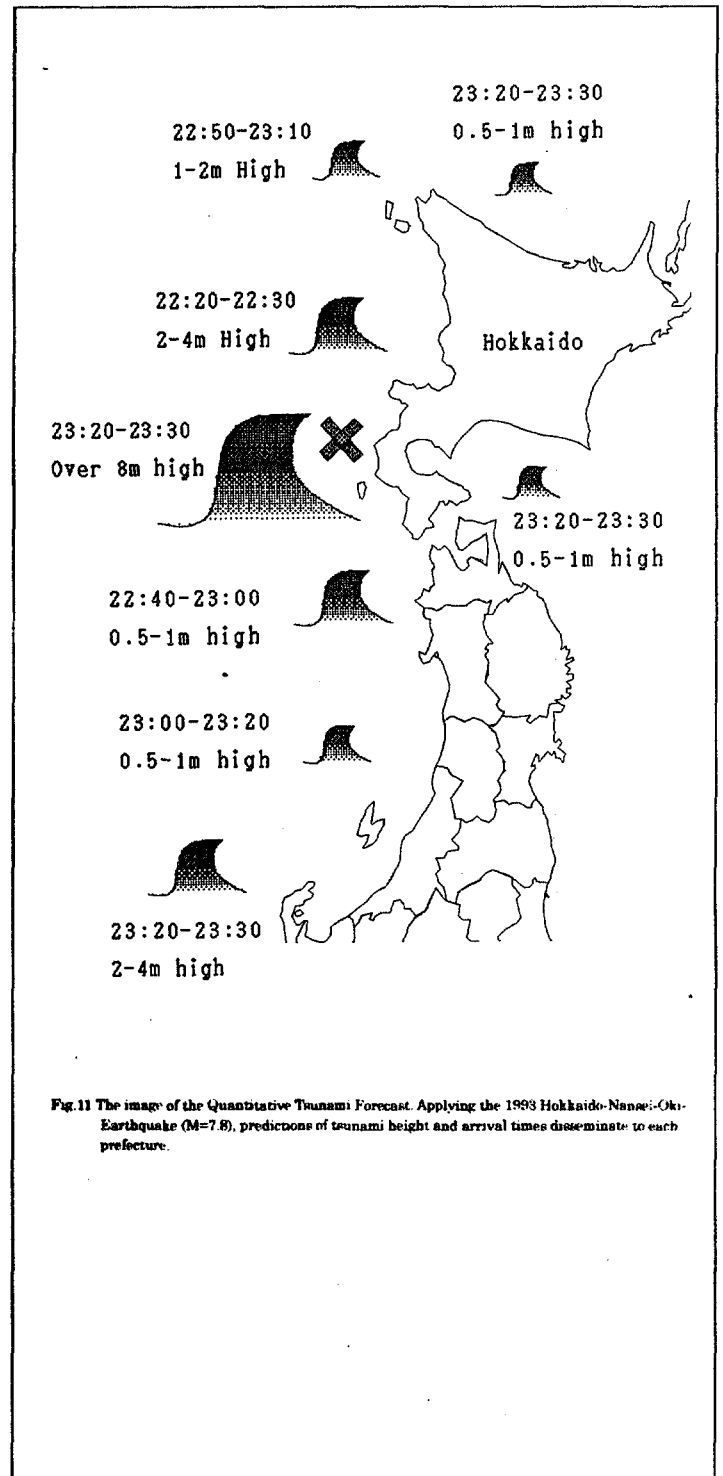
with this receiver.

5 Conclusion

To minimize tsunami disasters, the JMA has improved the tsunami forecasting system. A new seismograph network with 150 stations was constructed, and P-wave magnitude has been adapted for rapid determination of the hypocenter and magnitude. For rapid transmission of the warning/information, the new dissemination and receiving system using GMS has been developed also.

The present projects are to equip the tsunami forecast system with the Interpolation Numerical Tsunami Model. The JMA is going to disseminate the Quantitative Tsunami Forecast by 1999. Thus, in addition to today's GMS information, we will send more important information,

⑥ Prediction of tsunami arrival times,

⑦ Prediction of tsunami heights,

as Fig.11.

Fig. 11 The image of the Quantitative Tsunami Forecast. Applying the 1993 Hokkaido-Nansei-Oki Earthquake (M=7.8), predictions of tsunami height and arrival times disseminate to each prefecture.

6 Acknowledgments

References

Abe, Ku., 1978, A dislocation model of the 1933 Sanriku earthquake consistent with
the tsunami waves. J.Phys.Earth, 26, 381-396.

Charles L.Mader, George Curtis, 1991, Modeling Hilo, Hawaii Tsunami Inundation, Science of
Tsunami Hazard, Vol. 9, No 2, 85-94

Isamu Aida, Numerical experiments for the tsunami propagation 'The 1964 Niigata tsunami
and the 1968 Tokachioki tsunami', Bull.Earthq.Res.Inst., 47, 673-700.

Isamu Aida, 1974, Numerical Computation of a Tsunami Based on a Fault Origin Model of an
Earthquake, Journal of Seismological Society of Japan, 27, 141-154.

Isamu Aida, 1974a,Relation between Tsunami Inundation Heights and Water Surface
Profiles on a 200m Depth Contour, Journal of Seismological Society of Japan, 27, 141-154.

Isamu Aida, 1977,Simulation of Large Tsunamis Occurring in the Past Off the Coast of the
Sanriku District, Bull.Earthq.Res.Inst., 52, 71-101.

Isamu Aida, 1978,Reliability of a tsunami source model derived from fault parameters,
J.Phys.Earth, 26, 57-73.

Isamu Aida, 1979, A source Model of the Tsunami accompanying the Tonankai Earthquake of
1944, Bull.Eartq.Res.Inst., 54,367-390.

Isamu Aida, 1981b, Numerical Experiments of Historical Tsunami Generated Off the Coast of
the Tokaido District, Bull.Earthq.Res.Inst., 56, 367-390.

Isamu Aida, 1984,A Source Model of the Tsunami accompanying the Central Japan Sea Earthquake of 1983, Bull.Earthq.Res.Inst., 59,93-104.

Ando,M., 1975, Source mechanisms and tectonic significance of historical earthquake along
the Nankai trough, Japan, Tectonophysics, 27,119-140.

Kajiura, 1970,Tsunami source, energy and the directivity of wave radiation,
Bull.Earthq.Res.Inst., 56, 415-440.

H.Kanamori, 1977, The energy release in great earthquakes, J.Geophs.Res., 82, 2981-2987.

H.Kanamori and D.Anderson, 1975, Theoretical basis of some empirical relations in
seismology, Bull.Seismol.Soc.Am., 65, 1073-1095.

Mansinha,L.and D.Smylie, 1971, The displacement fields of inclined faults,
Bull.Seismol.Soc.Am., 61, 1433-1440.

Matsuda.,T.,Ota,M.Ando and N.Yonekura, 1978, Fault mechanism and recurrence time of
major earthquake in southern Kanto district, Japan, as deduced from coastal terrace
data, Geolog.Soc.Am.Bull., 89, 1610-1618.

Matsura,M.,T.Iwasaki and Y.suzuki,1980,Staitical and dynamical study on faulting
mechanism of the 1923 Kanto earthquake, J.Phys.Earth, 28, 119-143.
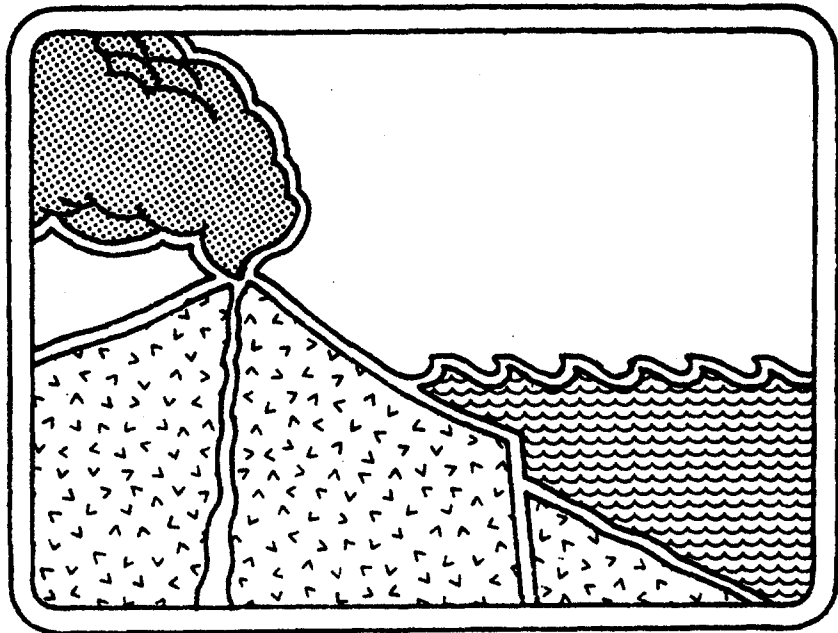
ELEVATION CHANGES ASSOCIATED WITH A TSUNAMIGENIC EARTHQUAKE

Shigehisa Nakamura
Famille Ville-A104, Tanabe 646-0031, Japan

ABSTRACT

The 1995 South Hyogo earthquake generated a small tsunami. Post earthquake geodetic surveys along the coast close to the epicenter showed elevation changes that apparently contradict a conventional notion of source mechanism, that the hypocenter is a point on a line formed by the intersection of two nodal planes. Research into earthquake source mechanism and tsunami source with emphasis on field data is recommended.

INTRODUCTION

Geodetic data from post-earthquake surveys of the 1995 South Hyogo Earthquake were studied to examine the actual process of a tsunamigenic earthquake. The shock was located in the Circum-Pacific seismic zone in the northwestern Pacific. The epicenter was several hundred kilometers west of the tectonic boundary between the Eurasian and Philippine Sea Plates. Several new faults appeared during the earthquake to produce elevation changes across the faults near the epicenter.

In this paper elevation changes found after the seismic event are studied in relation to the tsunamigenic earthquake. The data suggest that there is need to conduct tsunami research not on the basis of artificial models but investigations in terms of reasonable dynamics based on observed data.

PREVIOUS WORKS.

Environmental changes of the 1995 earthquake were studied (Nakamura, 1995; 1996a); the study was extended to include sea level changes brought about by the earthquake (Nakamura 1996b). Further studies monitored the local annual mean sea levels and the rising of the datum plane by comparing present changes with previous data sets (Nakamura 1990; 1993; 1994).

It should be noted that the epicenter of the 1995 South Hyogo Earthquake was located in a seismically active zone adjacent to one of the subduction zones (Bebout et al., 1996)..

EARTHQUAKE FAULTS FORMED BY THE EARTHQUAKE

For this study seismic records were obtained from seismic stations maintained by the Japan Meteorological Agency, but the author was not able to get hold of records of tsunamis and seiches generated by the earthquake. Figure 1 shows the epicenter "E" and the faults caused by the earthquake. Thick lines "F1" and "F2" are the faults newly formed in the earthquake. The faults were mapped by post-earthquake survey teams and were reported in a rapid publication from the Maritime Safety Agency. Several of the newly found faults (thin lines) are located out at sea under fine stratified sediments. It is diffuclt to consider that these faults were formed at the time of the main shock and contributed to tsunami generation.

After the earthquake the National Geographic Research Institute surveyed elevation changes along a line crossing the faults "F1" and "F2". The survey line H-K-S in Figure 1 started from Himeji (H), passed through Kobe (K), and ended at Osaka (S) along the coastline, veering close to the epicenter (E).

The elevation changes along line H-K-S are shown in Figure 2. The horizontal distance is not drawn according to scale. The diagram shows that significant upheaval occurrred between the two newly formed seismic faults "F1" and "F2". Source mechanism analyses, on the other hand, show that the epicenter and the tsunami source are located at the node of force distributions. The author wants to know what was the

process at the seismic source and questions the prevailing notions of earthquake source mechanism.

GEODETIC VARIATIONS AROUND THE EPICENTER.

The subduction process of the Pacific Plate and the Philippine Sea Plate beneath the Eurasian Plate is considered to be well known. Nevertheless, we have no information on the internal forces in the plates.

In the two years before the earthquake and the two years after the earthquake, the variations in annual mean sea level at tide stations located in the southern area of the tsunami source were synchronous. The variations at Kobe for 1995 were out of step from the other nearby tide stations.. Why such variations occurred should be investigated.

As Nakamura (1994) has pointed out, the annual mean sea level variations in the interested area are strongly influenced by Kuroshio known as the western boundary intensified currect in the northwestern Pacific. Further, only the author has paid attention to the submarine thermal variations that occurred fifteen minutes before the main shock of the 1995 South Hyogo Earthquake.

As there seems to be a correlation of mean sea level changes and tectonic processes, the author proposes that the pattern observed in the 1995 event can be understood not only in terms of seismic signals but also as a geodetic problem in plate tectonics. This might contribute to better understanding of tsunamigenic earthquakes in seismcally active zones adjacent to tectonic plate boundaries.

CONCLUSIONS

Using the data of the 1995 South Hyogo Earthquake, geodetic changes associated with a tsunamigenic earthquake were studied in relation to seismic fault formation. The elevation changes across the newly formed faults should be included in investigation of tsunamigenic earthquake process.

Bebout,G.E., D.W.Scoll,S.H.Kirby and J.P.Platt(eds.) 1996 Subduction-Top to Bottom, Geophysical Monograph 96 AGU, 384p.

Nakamura,S. 1990 Secular upheaval of datum level in relation to tsunamigenic earthquake, Marine Geodesy, Vol.14, pp.137-141.

Nakamura,S. 1993 Upheaval at tsunamigenic earthquakes in the northwestern Pacific, Marine Geodesy, Vol.16, pp.253-258.

Nakamura,S. 1994 Annual mean sea level variations in the northwestern Pacific seismic zone,Marine Geodesy,Vol.17 pp.213-218.

Nakamura,S. 1995 Oceanic subsurface thermal variations during the Hyogo South Earthquake, Sci.Tsunami Hazards (Int.J.Tsunami Soc.), Vol.13, pp.53-56.

Nakamura,S.1996a Possible environmental variations during an earthquake, Oceanology International 96 (OI96), Brighton UK, Vol.1, pp.333-340.

Nakamura,S. 1996b An extent of sea surface layer affected by an earthquake, Marine Geodesy, Vol.19, pp.281-289.

Nakamura,S. 1997 Interannual sea level variations neighbour the plates boundary, Conference Proc. of OI97 PACRIM, Singaore, Vol.1, pp.31-39.
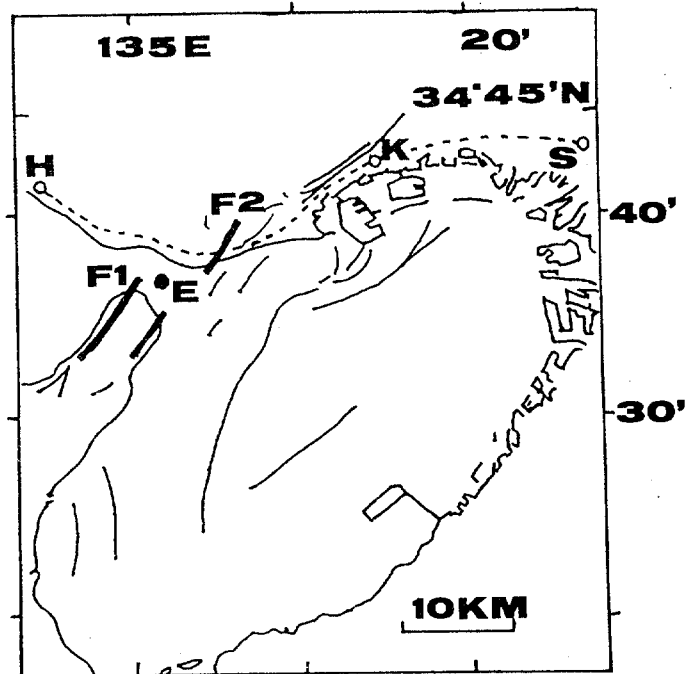
Figure 1.Locations of the epicenter of the 1995 Hyogo
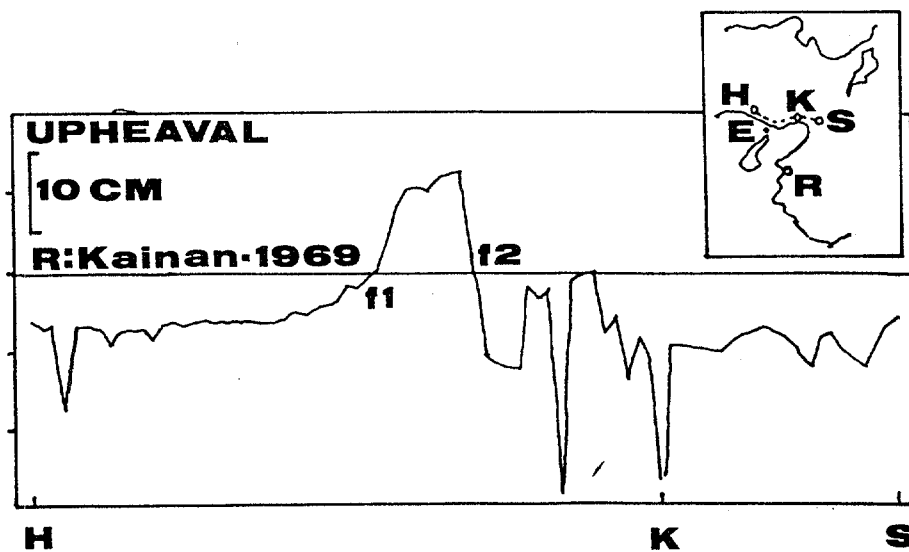   South Earthquake and of the seismic faults.

Figure 2.Remanent geodetic variations(upheavals) caused
        by the 1995 Hyogo South Earthquake along a
        survey line crossing the seismic faults just
        around the epicenter.

THE JULY 1998 NEW GUINEA TSUNAMI CARRIES BAD NEWS FOR HAWAII

Daniel A. Walker
Oahu Civil Defense Tsunami Advisor
59-530 Pupukea Road, Honolulu, HI 96712 USA

A recent article appearing in Science News [R. Monastersky, "Waves of Death: Why the New Guinea Tsunami Carries Bad News for North America," Science News, Vol 154-14, pages 221-223 (1998)] stated that the runup from the July 17, 1998 New Guinea tsunami reached 14 meters and more than 2,500 people were killed. The bad news suggested in the article is that locally generated tsunamis have struck, and will strike, portions of the West Coast of North America.

Tsunami researchers in Hawaii have individually over many years expressed concerns about locally generated tsunamis. The state of Hawaii has experienced a number of significant, locally generated tsunamis on the sparsely populated island of Hawaii. Two of these, in 1868 and 1975 had runups of about 14 meters, identical to that observed for the New Guinea tsunami.

Such earthquakes as the 1868 and 1975 events should not be viewed as only being possible along the Ka'u and Puna Coasts. Similar large events could occur along the Kona Coast (of the island of Hawaii). Modeling of a hypothetical Kalapana type earthquake off the Kona Coast suggests that tsunamis in excess of 10 feet, and perhaps comparable to the New Guinea values, could strike Oahu's south shore.

On the other hand with the current local warning threshold of 6.8 and an error of ± 0.5 units of magnitude, state-wide warnings may be called for earthquakes with magnitudes as low as 6.3. There have been about 9 local earthquakes with magnitudes of 6.3 or greater in this century (about 1 every 10 years). None of these have produced destructive tsunamis on islands other than the island of Hawaii.

In 1997 and 1998, meetings of all available tsunami researchers in Hawaii were held to provide consensus, rather than individual, advice to the State's Civil Defense Agency. These conclusions and recommendations are contained in two reports: *Recent Discussions Related to Tsunami Issues*" dated October 2, 1997 and *Conclusions and Recommendations Related to Local Tsunami Issues by Independent Tsunami Experts* dated May 21, 1998.

The following is a summary of the recommendations sent to the Hawaii Civil Defense based on the May 21, 1998 meeting.

The scientists and Civil Defense personnel attending this meeting recommended an immediate upgrade of PTWC's (Pacific Tsunami Warning Center) warning capability through:

1. The installation of additional coastal wave recorders on the Big Island (island of Hawaii) capable of providing real-time detection and warning of an impending tsunami.

2. The modeling of a suite of earthquakes around the Big Island with which future Big Island tsunamis can be matched.

3. Installation of open ocean wave gauges off the western coast of the Big Island. With modeling studies, such data would confirm that either a significant tsunami was on its way to other islands or no significant tsunami was about to strike other islands.

4. Coordinate and conduct a state wide public information/education campaign to better prepare island residents to cope with the local tsunami hazard.

In conclusion, it was agreed that without more instrumentation and modeling studies, there will continue to be unacceptably high risks of false local warnings, local warnings not issued in a timely manner, or missed local tsunamis. All of these possibilities would have serious consequences in terms of : (a) immediate or future injuries or fatalities, (b) the loss of credibility in Civil Defense agencies and the warning system, and (c) tourism.

The Hawaii tsunami scientists attending the meetings and contributing to the reports were Dr. Doak Cox, State Civil Defense Tsunami Advisor (Emeritus), Mr. George Curtis, Hawaii Civil Defense Tsunami Advisor, Dr. Augustine Furumoto, State Civil Defense Tsunami Advisor, Dr. Daniel Walker, Oahu Civil Defence Tsunami Advisor, Dr. Gerard Fryer, Dr. Donald Swanson, Dr. Charles McCreery, Mr. Michael Blackford, and Dr. Charles Mader.

REAL-TIME VISUAL OBSERVATIONS OF SMALL TSUNAMIS IN HAWAII GENERATED BY THE DECEMBER 5, 1997 KAMCHATKA EARTHQUAKES

Daniel A. Walker

Oahu Civil Defense Tsunami Advisor

59-530 Pupukea Road, Honolulu, HI 96712 USA

INTRODUCTION

Historically some of the largest runups reported in Hawaii for Pacific-wide tsunamis have been along Oahu's north shore. The largest statewide values were 4.9 meters at Waimea Bay from the Alaska earthquake of 1964 and 9.1 meters at Kaena Point from the Kamchatka earthquake of 1952. Largest Oahu values were 3.7 meters at Haleiwa in 1923 (Kamchatka), 7.0 meters at Kahuku in 1957 (Aleutians) and 4 meters near Mokuleia in 1960 (Chile). In addition, small tsunamis from the May 7, 1986 Aleutian and October 4, 1994 Kuril earthquakes, estimated to be less than 0.3 meters, were videotaped approximately one mile from the ocean as they traveled as a bore up Paukauila stream in the Waialua and Haleiwa area.

This history of strong responses to Pacific-wide tsunamis and the early morning cancellation of a December 5, 1997 tsunami watch for the 7.9 Mw Kamchatka earthquake, well in advance of its expected arrival time, suggested a unique opportunity for the safe observation of a small tsunami on Oahu's north shore.

OBSERVATIONS

Figure 1 is a photo taken from a bridge over Paukauila stream at about 7:30 a.m. Hawaiian time on December 5, 1997. The dark band across the stream is a sand bar produced by the opposing forces of the mountain stream emptying into Kaiaka Bay and small ocean waves moving upstream. The bridge seen in the picture is used to haul sugar cane. In some of the photos a large tractor can be seen at the eastern (right) edge of the bridge. The photo was taken because a small ripple emerged from the righthand side of the sand bar at a time corresponding to the expected arrival time of the first tsunami wave. The ripple can not be easily identified in the reproduction.

Figure 2 is a photo taken at about 8:00 a.m. as the sand bar became covered with water and small breaking waves. Powerful rapids began to move diagonally from right to left, from one bank of the stream to the other. This action generated the counter-clockwise whirpool about 30 meters in diameter shown in the lefthand central portion of the picture.

A corresponding clockwise whirpool then began to form further upstream. It grew to about 20 meters in diameter and is shown in Figure 3. The approximate 3 meter section of telephone pole shown in Figure 3 eventually moved upstream under the bridge from which the photos were taken and then headed back toward the ocean as the tsunami receded and the sand bar was once again exposed (Figures 4 and 5). Note the similarity of the surface smoothness of the stream in Figures 1, 4 and 5 as contrasted to the surface turbulence of Figures 2 and 3.

At about 8:20 another tsunami wave was observed and photographed. It was slightly smaller but had the same general characteristics of the 8:00 wave. The maximum runup

of the 8:00 wave was about 0.6 meters along the eastern (right) bank of the stream near the sandbar.

Returning home, the internet indicated that a 6.7 Mw aftershock occurred 7 hours and 21 minutes after the main shock. The question then arose as to whether it would be possible to see a tsunami from that earthquake in the quiet backwaters of Paukauila stream. The wave of the aftershock corresponding to the earlier 8:00 wave would arrive at 3:21 p.m. Two sticks were placed as markers into the mud near the water line along the bank of the stream, the time (3:17) was written in the mud, a 2 by 3 inch Civil Defence identification card was laid on the bank for scale and the picture shown in Figure 6 was taken. The water line slowly began to rise past the sticks and the number "3". The "17" was changed to a "29" to indicate the time, and the picture shown in Figure 7 was taken. The water line continued to rise, covering the number "2", and reached a maximum at 3:31. Once again the time was written in the mud and the photo shown in Figure 8 was taken. The estimated runup of this tsunami was 0.1 meter.

CONCLUSIONS

Extremely small tsunamis can be visually observed in quiet backwater areas which are along coastlines historically responsive to large Pacific-wide tsunamis.

I wish to thank Joe Reed for providing timely information on the watch cancellation, Francine Walker for assistance with the observations, and Napono Walker for help with the runup-survey.

Figure 1.

The quiet Paukauila stream sandbar, bridge and ocean at about 7:30 a.m. Hawaiian Standard Time on December 5, 1997.
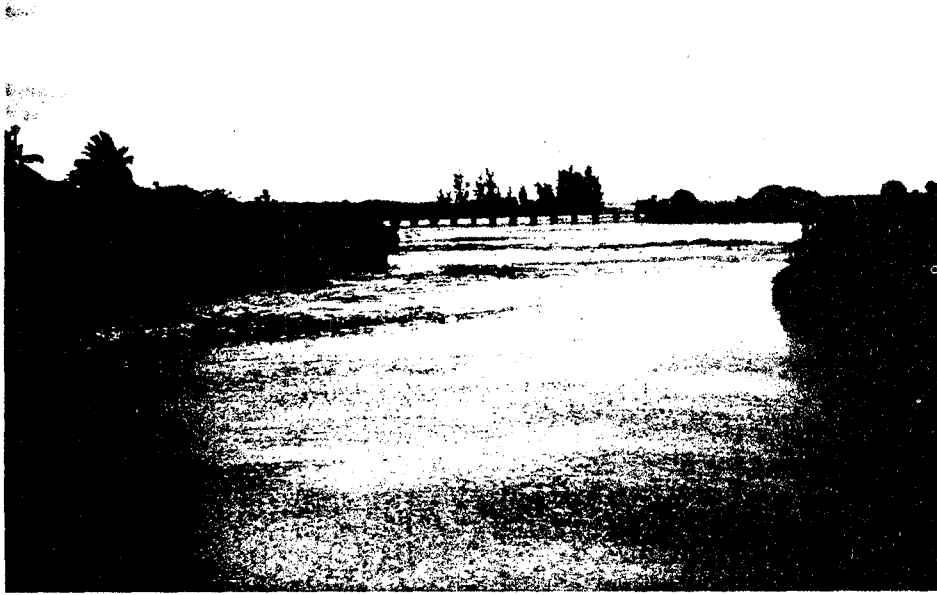
Figure 2.

At 8:00 a.m. the sandbar is covered by a tsunami and small breaking waves. Powerful rapids across the stream from the right bank near the sandbar to the left bank generated a 30 meter diameter, counter-clockwise whirlpool in the left center of the picture. The 7.9 Mw Kamchatka earthquake generated this tsunami.

Figure 3.

A clockwise whirlpool developed further upstream near the bridge from which the photos were taken. A 3 meter section of telephone pole moved upstream.
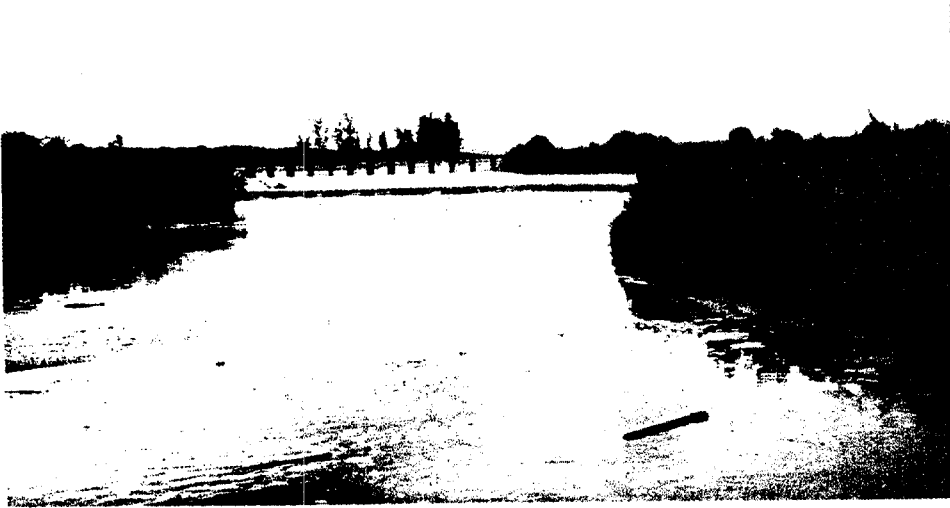
Figure 4.

The waters receded once again, exposing the sandbar and moving the pole downstream.

Figure 5.

The water continued to receed and the pole moved further downstream just below the middle of the sandbar.

Figure 6.

Markers before a possible mini-tsunami on December 5, 1997 at 3:17 p.m.

Figure 7.

Approaching the maximum runup of the mini-tsunami at about 3:29 p.m.

Figure 8.

Maximum runup of 0.1 meters observed at 3:31 p.m. from the 6.7 Mw Kamchatka earthquake.

The

𝕿𝖘𝖚𝖓𝖆𝖒𝖎 𝕾𝖔𝖈𝖎𝖊𝖙𝖞 𝕬𝖜𝖆𝖗𝖉

FOR LONG TERM CONTRIBUTIONS TO

TSUNAMI SCIENCE

Presented to:

JAMES LANDER

At the 7th International Conference
on Natural and Man-Made Hazards,
Chania, Greece, May 1998

George Curtis, President, the Tsunami Society

APPLICATION FOR MEMBERSHIP

THE TSUNAMI SOCIETY
P. O. Box 25218
Honolulu, Hawaii 96825, USA

I desire admission into the Tsunami Society as: (Check appropriate box.)

☐ Student   ☐ Member   ☐ Institutional Member

Name _____Signature _____

Address _____Phone No. _____

_____

Zip Code _____Country _____

Employed by _____

Address _____

Title of your position _____

FEE: Student $5.00   Member $25.00   Institution $100.00

Fee includes a subscription to the society journal: SCIENCE OF TSUNAMI HAZARDS.

Send dues for one year with application. Membership shall date from 1 January of the year in which the applicant joins. Membership of an applicant applying on or after October 1 will begin with 1 January of the succeeding calendar year and his first dues payment will be applied to that year.